

Hybrid Feedback-Guided Optimal Learning for Wireless Interactive Panoramic Scene Delivery

Xiaoyi Wu, Graduate Student Member, IEEE, Juaren Steiger, Member, IEEE, Bin Li, Senior Member, IEEE and R. Srikant, Fellow, IEEE

Abstract—Immersive applications such as virtual and augmented reality impose stringent requirements on frame rate, latency, and synchronization between physical and virtual environments. To meet these requirements, an edge server must render panoramic content, predict user head motion, and transmit a portion of the scene that is large enough to cover the user viewport while remaining within wireless bandwidth constraints. Each portion produces two feedback signals: prediction feedback, indicating whether the selected portion covers the actual viewport, and transmission feedback, indicating whether the corresponding packets are successfully delivered. Prior work models this problem as a multi-armed bandit with two-level bandit feedback, but fails to exploit the fact that prediction feedback can be retrospectively computed for all candidate portions once the user head pose is observed. As a result, prediction feedback constitutes full-information feedback rather than bandit feedback. Motivated by this observation, we introduce a two-level hybrid feedback model that combines full-information and bandit feedback, and formulate the portion selection problem as an online learning task under this setting. We derive an instance-dependent regret lower bound for the hybrid feedback model and propose AdaPort, a hybrid learning algorithm that leverages both feedback types to improve learning efficiency. We further establish an instance-dependent regret upper bound that matches the lower bound asymptotically, and demonstrate through real-world trace driven simulations that AdaPort consistently outperforms state-of-the-art baseline methods.

I. Introduction

The evolution of immersive technologies, including extended reality (XR), which includes both virtual reality (VR) and augmented reality (AR), holographic displays, and volumetric capture, is redefining digital interaction across multiple domains, such as gaming, telepresence, remote collaboration, and immersive training. These systems provide users with highly responsive and interactive virtual environments that continuously adapt to their movements and perspectives in real time. In practical deployments, panoramic visual content is commonly streamed wirelessly from an edge server to a head-mounted display (HMD), such as a VR headset, since strict weight and power constraints limit the onboard rendering capabilities of HMDs for high-fidelity 3D graphics. Unlike traditional video streaming, immersive panoramic experiences are particularly sensitive to latency and misalignment, which may result in user discomfort or motion sickness. To ensure a seamless experience, tight synchronization between the

user's real-world head pose (i.e., position and orientation) and the corresponding virtual viewpoint is essential. Consequently, the edge server cannot rely solely on the latest pose information and must instead predict the user's current head pose. Based on this prediction, the server proactively transmits a region of the panoramic scene that is sufficiently large to fully cover the user's viewport, while compensating for inevitable head-motion prediction errors.

A straightforward approach would be for the edge server to transmit a portion covering the full 360° panoramic scene. However, such a strategy is impractical due to constraints imposed by the wireless channel and stringent real time streaming requirements. Compared to conventional video delivery, panoramic video streaming typically demands four to six times higher bandwidth [1]. As a result, transmitting the entire scene can easily cause severe congestion. Moreover, user interaction in immersive panoramic environments induces frequent and rapid head movements, which in turn lead to more pronounced channel dynamics than those experienced by stationary users. This increased variability further exacerbates packet loss. Real time latency constraints also play a critical role. For instance, Meta recommends a target of 60 frames-per-second (FPS) for media applications, while interactive applications are required to sustain at least 72 FPS on Meta Quest headsets [2]. In addition, user studies conducted by Wang et al. [3] indicate that frame rates around 120 FPS significantly reduce virtual reality sickness. Under such stringent timing requirements, the edge server often lacks sufficient opportunity to retransmit lost packets within a single frame interval. Consequently, the server must carefully select a transmission region that is large enough to reliably cover the user viewport, yet sufficiently small to be delivered successfully over the wireless channel within one frame duration.

If the dynamics of the user's head motion and the wireless channel were known in advance, the edge server could calculate the optimal delivery portion. However, in practice, these statistics are unknown and must be learned in real-time. A natural approach is to model the problem as a multi-armed bandit, where each arm is a delivery portion and a Bernoulli reward is accrued in a timeslot if the chosen delivery portion results in the user successfully seeing their entire viewport. In general, the rewards are non-i.i.d. due to the nonstationary user head motion and

panoramic content. However, stochastic bandit algorithms, such as KL-UCB, are shown to empirically converge in real-world panoramic scene delivery experiments [4]. Moving beyond this basic formulation, Chen et al. [5] observe that the overall reward naturally decomposes into two distinct feedback signals. The first corresponds to the prediction outcome, which captures whether the selected delivery portion indeed covers the user actual viewport. The second corresponds to the transmission outcome, which reflects whether all packets associated with the selected portion are successfully delivered over the wireless channel. In their framework, prediction and transmission outcomes are treated as separate bandit feedback observations, leading to what they term “two-level bandit feedback”. Throughout this paper, we denote this setting as 2/B/B, while the conventional single-level bandit feedback is denoted as 1/B.¹ In the presence of two underlying bandit feedback signals, the 1/B setting corresponds to the scenario in which only the product of the two feedback signals is observable.

However, existing works [4], [5] overlook an important structural property of the problem. Once the edge server receives the user head pose, it can retrospectively determine whether the user viewport would have been covered by every possible delivery portion, rather than only the portion selected in the previous time slot. As a result, the prediction outcome is not a bandit signal but instead constitutes full-information feedback. The learning problem therefore exhibits two-level feedback in which one level provides full-information feedback and the other provides bandit feedback. We refer to this feedback structure as 2/F/B. In this paper, we investigate how exploiting this richer feedback structure can improve learning efficiency for wireless interactive panoramic scene delivery. In particular, we demonstrate the advantages of leveraging 2/F/B feedback over conventional 2/B/B and 1/B feedback models. Our main contributions are summarized as follows:

- 1) We formulate the problem of maximizing cumulative successful viewport delivery of an interactive panoramic scene as an online learning problem with two-level full-information and bandit (2/F/B) feedback. To our knowledge, this formulation involving mixed feedback types is novel and has not been explored previously in a theoretical or practical setting in the literature.
- 2) We derive an instance-dependent lower bound on the regret under 2/F/B feedback (Theorem 1), which is shown to be significantly smaller than the corresponding lower bounds for 2/B/B and 1/B feedback for some problem instances. This suggests that incorporating

¹This $n/x/x$ notation, where n indicates the number of different feedback signals, and the remaining x 's indicate the type of each feedback signal, is inspired by Kendall's notation from queueing theory.

full-information feedback can significantly improve learning efficiency.

- 3) We design the Hybrid Feedback-Driven Learning for Adaptive Portion Selection (AdaPort) algorithm: a novel online learning algorithm that leverages 2/F/B feedback by using the empirical mean estimate for the full-information feedback and the Thompson sample for the bandit feedback.
- 4) We derive an instance-dependent upper bound (Theorem 2) for AdaPort that matches the lower bound asymptotically, thus showing that the algorithm is asymptotically optimal. We also verify the improved theoretical performance compared to prior algorithms using 2/B/B and 1/B feedback by conducting numerical simulations.
- 5) To validate the practical effectiveness of AdaPort, we perform simulations using a real-world data trace consisting of user head motion, panoramic video content and wireless transmission bandwidth. Our results show that AdaPort consistently outperforms state-of-the-art stochastic bandit portion selection algorithms that use 2/B/B and 1/B feedback. It is also shown to outperform the EXP3 algorithm with 1/B feedback for adversarial bandits.

This work extends our conference version [6] in the following aspects: (1) more detailed proofs for Theorem 1 and Theorem 2 are included; (2) we collect more real-world data traces and conduct additional simulations to showcase the superior performance of our algorithm.

Note on Notation: We use bold and script font of a variable to denote a vector and a set, respectively. We use $a \wedge b$ to denote the $\min\{a, b\}$. We use $[N] \triangleq \{1, 2, \dots, N\}$ to denote the set of the first N positive integers. We use $f(x) = o(g(x))$ to denote that $\lim_{x \rightarrow \infty} f(x)/g(x) = 0$, and $f(x) = O(g(x))$ to denote that $\limsup_{x \rightarrow \infty} f(x)/g(x) < \infty$, for positive functions f and g . We write $f(x) = \Theta(g(x))$ if there exist constants $c_1, c_2 > 0$ and x_0 such that $c_1 g(x) \leq f(x) \leq c_2 g(x)$ for all $x \geq x_0$. $F_{n,p}^B(\cdot)$ denotes the cumulative distribution function (CDF) of the binomial distribution with n trials and success probability p . We use $\text{Beta}(\alpha, \beta)$ to denote the Beta distribution with parameters α and β and $F_{\alpha, \beta}^{\text{Beta}}(\cdot)$ to denote the CDF of this Beta distribution. $d(p_1, p_2) \triangleq p_1 \log\left(\frac{p_1}{p_2}\right) + (1 - p_1) \log\left(\frac{1 - p_1}{1 - p_2}\right)$ is the KL-divergence between the Bernoulli(p_1) and Bernoulli(p_2) distributions. 1/B refers to the standard (one-level) bandit feedback, 2/B/B refers to two-level bandit feedback, and 2/F/B refers to two-level feedback where one level is full-information, and the other level is bandit feedback.

II. related work

In this section, we review the related work on interactive panoramic scene delivery, and on online learning under full-information feedback and under bandit feedback.

A. Interactive Panoramic Scene Delivery

Panoramic scene delivery places significantly greater demands on network bandwidth than traditional video streaming. To address these challenges and enhance user experience, numerous studies have explored strategies for optimizing panoramic content transmission (e.g., [7], [8]). For example, Qian et al. [8] introduced an adaptive scheme that transmits only the portion of the panoramic scene aligned with the predicted user viewport, effectively reducing bandwidth consumption. However, these early approaches primarily relied on heuristic methods without providing theoretical performance guarantees. In response, subsequent research has introduced multi-armed bandit frameworks to the problem of panoramic scene delivery, aiming to provide a more principled and theoretically grounded understanding. Notably, recent studies have begun to explore how to effectively utilize the two distinct feedback signals inherent in this setting: motion prediction and wireless transmission. For example, Chen et al. [5] proposed the Two-Level Thompson Sampling algorithm to optimize viewport selection and maximize system throughput, while Gupta et al. [4] developed a Two-Level KL-UCB approach for the same objective. In parallel, other works have addressed multi-user scenarios (e.g., [9]–[11]) and multi-objective learning (e.g. [12]) in panoramic scene delivery. Nevertheless, prior studies have generally overlooked a key observation: the prediction outcome provides a full-information feedback signal, while the wireless transmission outcome yields bandit feedback. Thus, the problem naturally exhibits a two-level hybrid feedback structure, combining both full-information and bandit feedback, which has not been explicitly modeled or exploited in existing work.

B. Full-information and Bandit Feedback

In the online learning setting, bandit feedback refers to the scenario where the player observes the reward only for the arm selected at each timeslot, while the rewards of all other actions remain unobserved. In contrast, full-information feedback provides the player with the rewards of all available arms at each timeslot, regardless of the action selected. This richer feedback enables more informed learning strategies. In the context of bandit feedback, several classical algorithms have been extensively studied, including UCB [13], KL-UCB [14], and Thompson Sampling [15]. While most foundational work focuses on this bandit feedback setting, there also exist a number of studies exploring full-information feedback in both stochastic and non-stochastic bandit frameworks (e.g., [16]–[21]). For instance, Zhao et al. [16] examined a one-sided full-information stochastic bandit problem, where selecting an arm yields a reward from an unknown distribution while also revealing feedback from all arms located on one side of the selected arm. Alon et al. [17] introduced a partial-information model for online learning

that generalizes and interpolates between the classical full-information and bandit settings. However, to the best of our knowledge, existing literature does not address the hybrid feedback setting where the player receives both full-information feedback and bandit feedback simultaneously within an online learning setting.

III. System Model

We consider a system in which a single user interacts with an immersive panoramic scene that is delivered wirelessly from an edge server. The panoramic scene can be conceptualized as video content projected onto the inner surface of a virtual sphere surrounding the user's head. The user's viewport, i.e., the visible portion of the scene, which typically constitutes around 20% of the sphere's surface, is a rectangle centered at a fixed origin point corresponding to the user's view direction. The content on the sphere's surface changes as the user moves through the scene and rotates their head, and also changes according to the dynamics of the virtual environment. Using a standard map projection technique, such as equirectangular projection, the spherical panoramic content is transformed into a two-dimensional finite grid of tiles². A delivery portion is a rectangular formation of tiles centered at and with dimensions larger than the user's viewport. We assume there are N fixed delivery portions that the edge server can choose from in each timeslot. Note that each timeslot $t = 1, 2, \dots$ corresponds to a video frame and the system operates at 60-120 timeslots per second depending on the application's framerate requirement.

A. Online Learning under 2/F/B Feedback

After the edge server selects the delivery portion $i(t) \in [N]$ in timeslot t , the content corresponding to that delivery portion is sent to the user as a sequence of packets. Note that in general, the content may not be predetermined and may be updated in real-time according to the user's inputs (e.g., consider a VR video game). Therefore, we can only use a limited playback buffer because the content in timeslot t may become immediately irrelevant in timeslot $t+1$. Therefore, the content occupying the user's viewport in timeslot t must be sent from the server and received by the user by the end of timeslot t . Additionally, due to the short timeslot length, we do not consider any packet retransmissions. However, we assume a packet sent from the user to the edge server, called the ACK packet, containing the transmission acknowledgment, head pose, and other inputs from the previous timeslot is small enough that it can be reasonably assumed to be reliably delivered.

1) Prediction Outcome as Full-Information Feedback: At the beginning of timeslot $t+1$, the server will have received the user's ACK packet from timeslot t . Therefore, the server knows the user's predicted head pose, as well as their actual head pose from timeslot t , and can

²A tile represents the atomic unit for image encoding/decoding.

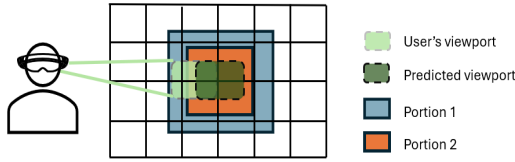


Fig. 1: Relationship between the user's viewport, the predicted viewport, and delivery portions.

calculate whether or not each portion $i \in [N]$ would have covered their viewport. We use $X_i(t) = 1$ to indicate that portion i can cover the user's viewport in timeslot t and $X_i(t) = 0$ otherwise. As illustrated in Fig.1, given the user's actual viewport (light green), portion 1 fully covers it, i.e., $X_1(t) = 1$, whereas portion 2 does not, i.e., $X_2(t) = 0$. Then the server observes the entire vector $\mathbf{X}(t) \triangleq (X_i(t))_{i=1}^N$ by the beginning of timeslot $t+1$, i.e. the server receives full-information feedback for the prediction outcome. We assume $\mathbf{X}(t)$ is i.i.d. over time and each component has unknown rate $\alpha_i \triangleq \mathbb{E}[X_i(t)]$. However, note that $\mathbf{X}(t)$ is component-wise dependent, i.e. for a fixed timeslot t and two portions $i \neq j$, $X_i(t)$ and $X_j(t)$ are not independent. As previously mentioned, they are actually both functions of two random variables, namely, the edge server's prediction of the user's head pose from timeslot t and the user's actual head pose from timeslot t .

2) Transmission Outcome as Bandit Feedback: At the beginning of timeslot $t+1$, after receiving the user's ACK packet from timeslot t , the server knows whether or not the transmission of delivery portion $i(t)$ was successful. We use $Y_i(t) = 1$ to indicate a successful transmission when delivery portion $i(t) = i$ is selected, and $Y_i(t) = 0$ otherwise. Then the server observes the transmission outcome $Y_{i(t)}(t)$ as bandit feedback. In this paper, we consider the transmission to have failed if any packet constituting the delivery portion $i(t)$ is lost. However, the problem can easily be extended to consider a failed transmission to occur only when a minimum portion of the packets are lost. As with the prediction outcome, we assume $\mathbf{Y}(t) \triangleq (Y_i(t))_{i=1}^N$ is i.i.d. over time, but unlike the prediction outcome, was assume it is component-wise independent, with each component having an unknown rate $\beta_i \triangleq \mathbb{E}[Y_i(t)]$. Note that, as illustrated in Fig.1, all candidate portions encompass the predicted viewport (dark green), being centered on it and expanded outward to varying extents. We also assume that for a fixed portion i and timeslot t , $X_i(t)$ and $Y_i(t)$ are independent.

We use $Z_i(t) = 1$ to indicate that the user can successfully view the desired content when portion $i(t) = i$ is selected in timeslot t , and $Z_i(t) = 0$ otherwise. We also refer to $Z_i(t)$ as the "throughput" or "reward" for portion i in timeslot t . Note that $Z_i(t) = 1$ only when both the prediction and the transmission are successful, i.e. $Z_i(t) = X_i(t)Y_i(t)$. Our objective is to design an adaptive portion selection algorithm that maximizes the

expected cumulative throughput $\sum_{t=1}^T \mathbb{E}[Z_{i(t)}(t)]$ up to a time horizon T when the prediction and transmission rates $(\alpha_i, \beta_i)_{i=1}^N$ are unknown. If the parameters were known, the optimal policy would be to always play the arm $i^* \in \arg \max_{i \in [N]} \alpha_i \beta_i$. Therefore, the regret is given by

$$\begin{aligned} R(T) &\triangleq \sum_{t=1}^T \mathbb{E}[Z_{i^*}(t) - Z_{i(t)}(t)] \\ &= T\alpha_{i^*}\beta_{i^*} - \sum_{t=1}^T \mathbb{E}[X_{i(t)}(t)Y_{i(t)}(t)] \\ &= \sum_{i \neq i^*} \Delta_i \mathbb{E}[n_i(T)], \end{aligned} \quad (1)$$

where $\Delta_i \triangleq \alpha_{i^*}\beta_{i^*} - \alpha_i\beta_i$ denotes the reward gap for portion i and $n_i(T) \triangleq \sum_{t=1}^T \mathbb{1}\{i(t) = i\}$ denotes the number of plays of portion i up to timeslot T .

To summarize, adaptive portion selection for wireless interactive panoramic scene delivery under 2/F/B feedback proceeds as follows: In each timeslot t ,

- ① The server decides the delivery portion $i(t)$ for timeslot t according to its history of observations $(\mathbf{X}(\tau), Y_{i(\tau)}(\tau), i(\tau))_{\tau=1}^{t-1}$.
- ② The server predicts the user's head pose for timeslot t and sends the content occupying the chosen delivery portion $i(t)$ centered on the user's predicted head pose to the user over the wireless channel.
- ③ The server receives the ACK packet for timeslot t and observes the user's actual head pose and the transmission outcome $Y_{i(t)}(t)$.
- ④ The server calculates the prediction outcome $X_i(t)$ for each portion i from the user's actual head pose (received in the ACK packet) and the server's predicted head pose.

B. Comparison with 1/B and 2/B/B Feedback

Using the language of the multi-armed bandit literature, we sometimes call a delivery portion $i \in [N]$ an "arm". For a bandit feedback signal, balancing exploration and exploitation is crucial. That is, exploring underplayed arms vs. exploiting the current most promising arm. The prior work on portion selection [4], [5] improved on the 1/B feedback model, where the edge server only receives the throughput $Z_{i(t)}(t)$ as feedback, by considering the 2/B/B feedback model, where the edge server receives both $X_{i(t)}(t)$ and $Y_{i(t)}(t)$ as feedback. While 2/B/B gathers more information per timeslot, both feedback signals are bandit, and are therefore subject to the exploration/exploitation dilemma. The major improvement we introduce with the 2/F/B feedback model is to completely remove the necessity for exploration in one of the feedback signals. Also note that 2/F/B feedback yields $N - 1$ more pieces of information compared to 2/B/B feedback.

C. Discussion and Limitation

In this subsection, we discuss the limitations of the assumptions in our system model. Specifically, we assume that $\mathbf{X}(t)$ and $\mathbf{Y}(t)$ are i.i.d. over time, and that $\mathbf{X}(t)$ and $\mathbf{Y}(t)$ are independent. These assumptions, also adopted in [4], [5], facilitate analytical tractability. In practice, however, $\mathbf{X}(t)$ may exhibit temporal dependencies due to user head movements, violating the i.i.d. assumption, while $\mathbf{Y}(t)$ may deviate from i.i.d. behavior due to variations in the panoramic scene content. Furthermore, $\mathbf{X}(t)$ and $\mathbf{Y}(t)$ may be dependent because recent head poses can be related to the scene content. Recall that we also assumed $\mathbf{Y}(t)$ is component-wise independent. However, in reality, if we successfully deliver the chosen portion, then we know that we could have also successfully delivered a smaller portion, and if we fail to deliver the chosen portion, then we know that we would have also failed to deliver a larger portion. Despite these modeling assumptions, it is worth noting that our real-world trace-based evaluations, which do not rely on any i.i.d. or independence assumption, show that the proposed algorithm consistently outperforms baseline methods. Finally, we note that the 2/F/B feedback model is of independent theoretical interest beyond the 2/B/B model studied in [4], [5].

IV. Algorithm Design

Recall the step-by-step summary of the sequence of events for the adaptive portion selection problem under 2/F/B feedback presented in Section III. In this section, we focus on step ①. Specifically, how to design an adaptive portion selection algorithm to select the delivery portion $i(t)$ in timeslot t given the history of observations $(\mathbf{X}(\tau), Y_{i(\tau)}(\tau), i(\tau))_{\tau=1}^{t-1}$. Recall that the optimal policy always selects $i^* \in \arg \max_{i \in [N]} \alpha_i \beta_i$ in each timeslot t . Since $(\alpha_i, \beta_i)_{i=1}^N$ are unknown, we instead choose

$$i(t) \in \arg \max_{i \in [N]} \bar{\alpha}_i(t) \theta_{\beta,i}(t). \quad (2)$$

where each $\bar{\alpha}_i(t)$ and $\theta_{\beta,i}(t)$ are our best estimates of α_i and β_i respectively, estimated from the history of observations. The details of how these estimates are chosen are given in the following subsections, and our algorithm, AdaPort is given in Algorithm 1.

A. Prediction Rate Estimate

Recall that the prediction outcome is a full-information feedback signal. Then to estimate α_i for each portion $i \in [N]$, we simply use the empirical mean $\bar{\alpha}_i(t) \triangleq \frac{1}{t-1} \sum_{\tau=1}^{t-1} X_i(\tau)$ for timeslots $t > 1$ and $\bar{\alpha}_i(1) = 0$ (the value of $\bar{\alpha}_i(1)$ is arbitrary under full-information). This estimate can be updated iteratively using the recurrence

$$\bar{\alpha}_i(t+1) = \bar{\alpha}_i(t) + \frac{1}{t} (X_i(t) - \bar{\alpha}_i(t)). \quad (3)$$

B. Transmission Rate Estimate

Unlike the prediction outcome signal, the transmission outcome is a bandit feedback signal. Therefore, we need to use an estimate of each β_i that is able to balance exploration and exploitation. Following [5], we adopt a Bayesian approach based on Thompson Sampling to estimate the transmission rate. Under Thompson Sampling, the estimate $\theta_{\beta,i}(t)$ is drawn from a prior distribution representing our current belief about the unknown parameter β_i . For Bernoulli rewards, we draw the Thompson sample $\theta_{\beta,i}(t) \sim \text{Beta}(S_{\beta,i}(t) + 1, F_{\beta,i}(t) + 1)$, where $S_{\beta,i}(t)$ and $F_{\beta,i}(t)$ denote the number of observed transmission successes and failures respectively. These are initialized as $S_{\beta,i}(1) = 0$ and $F_{\beta,i}(1) = 0$ and updated as

$$\begin{aligned} S_{\beta,i}(t+1) &= S_{\beta,i}(t) + \mathbf{1}\{i(t) = i\} Y_{i(t)}(t), \text{ and} \\ F_{\beta,i}(t+1) &= F_{\beta,i}(t) + \mathbf{1}\{i(t) = i\} (1 - Y_{i(t)}(t)). \end{aligned} \quad (4)$$

Exploration of each portion i is accomplished in Thompson sampling due to the variance in the Beta distribution, which shrinks as the number of plays $n_i(t)$ of portion i increases.

Algorithm 1 Hybrid Feedback-Driven Learning for Adaptive Portion Selection Algorithm (AdaPort)

```

1: Initialization: Set  $S_{\beta,i}(1) = F_{\beta,i}(1) = \bar{\alpha}_i(1) = 0 \quad \forall i \in [N]$ .
2: for each  $t = 1, 2, \dots$  do
3:   for each portion  $i$  do
4:     Draw  $\theta_{\beta,i}(t) \sim \text{Beta}(S_{\beta,i}(t) + 1, F_{\beta,i}(t) + 1)$ .
5:   end for
6:   Send the delivery portion  $i(t) \in \arg \max_i \bar{\alpha}_i(t) \theta_{\beta,i}(t)$ .
7:   Receive the feedback  $(\mathbf{X}(t), Y_{i(t)}(t))$ .3
8:   for each portion  $i$  do
9:     Update  $\bar{\alpha}_i(t)$  according to (3).
10:    Update  $S_{\beta,i}(t)$  and  $F_{\beta,i}(t)$  according to (4).
11:   end for
12: end for

```

V. Performance Analysis

In this section, we begin by deriving the regret lower bound for the online learning problem with 2/F/B feedback. We then compare this lower bound against the known lower bounds for 2/B/B feedback derived by Gupta et al. [4] and for 1/B feedback derived by Lai and Robbins [22]. To further support our motivation, we present simple illustrative examples that highlight the significant improvement in the lower bound under the 2/F/B feedback setting. Finally, we establish the regret upper bound of AdaPort (Algorithm 1), which matches the lower bound asymptotically.

³Refer to steps (3) and (4) in the step-by-step summary of events in Section III.

A. Regret Lower Bound under 2/F/B Feedback

In the following theorem, we present our asymptotic instance-dependent regret lower bound for online learning under 2/F/B feedback.

Theorem 1. (Lower bound) Consider an online learning algorithm under 2/F/B feedback that achieves $R(T) = o(T^\delta) \ \forall \delta > 0$. Then the algorithm is subject to the following regret lower bound:

$$\liminf_{T \rightarrow \infty} \frac{R(T)}{\log T} \geq \sum_{i \neq i^* : \alpha_i > \alpha_{i^*} \beta_{i^*}} \frac{\Delta_i}{d\left(\beta_i, \frac{\alpha_{i^*} \beta_{i^*}}{\alpha_i}\right)}. \quad (5)$$

Proof. Recall from (1) that the regret can be decomposed as $R(T) = \sum_{i \neq i^*} \Delta_i \mathbb{E}[n_i(T)]$. Then it suffices to show that $\liminf_{T \rightarrow \infty} \frac{n_i(T)}{\log T} \geq \frac{1}{d\left(\beta_i, \frac{\alpha_{i^*} \beta_{i^*}}{\alpha_i}\right)}, \forall i \in \mathcal{I}$, where $\mathcal{I} \triangleq \{i \neq i^* : \alpha_i > \alpha_{i^*} \beta_{i^*}\}$. Given arm $j \in \mathcal{I}$, fix $\lambda \in (\Delta_j, \alpha_j(1-\beta_j))$. We construct a new problem instance given by a second set of parameters $(\alpha'_i, \beta'_i)_{i=1}^N$ where $(\alpha'_i)_{i=1}^N = (\alpha_i)_{i=1}^N$, $\beta'_j = \beta_j + \lambda/\alpha_j$, and $\beta'_i = \beta_i$ for all $i \neq j$. The remainder of the proof is similar to the usual instance-dependent lower bound for stochastic bandits (see e.g. Theorem 16.2 in [23]), with some slight modifications to account for the two levels of feedback. The full proof can be found in Appendix A. \square

The right-hand side of (5) is called the “lower bound constant”. A key observation about the bound in Theorem 1 is that arms with $\alpha_i \leq \alpha_{i^*} \beta_{i^*}$ have zero contribution to the lower bound constant. This shows that an optimal algorithm (i.e., one with matching upper bound) in this setting only requires a constant number of plays to determine that these arms are suboptimal, whereas optimal algorithms in the 2/B/B and 1/B feedback regimes require a continual $\log T$ number of plays of each suboptimal arm. Intuitively, when $\alpha_i \leq \alpha_{i^*} \beta_{i^*}$, even if the transmission rate of the suboptimal arm i is 1, it is unlikely that this arm i can compete with the optimal arm.

Remark 1 (lower bound constant comparison).

$$\begin{aligned} & \overbrace{\sum_{\substack{i \neq i^* : \\ \alpha_i > \alpha_{i^*} \beta_{i^*}}} \frac{\Delta_i}{d\left(\beta_i, \frac{\alpha_{i^*} \beta_{i^*}}{\alpha_i}\right)}}^{\text{2/F/B lower bound constant}} \\ &= \sum_{\substack{i \neq i^* : \\ \alpha_i > \alpha_{i^*} \beta_{i^*}}} \frac{\Delta_i}{d(\alpha_i, x_i) + d(\beta_i, y_i)}, \quad x_i = \alpha_i, \quad y_i = \frac{\alpha_{i^*} \beta_{i^*}}{\alpha_i} \\ &\leq \sum_{\substack{i \neq i^* : \\ \alpha_i > \alpha_{i^*} \beta_{i^*}}} \frac{\Delta_i}{\min_{\substack{0 \leq x_i, y_i \leq 1 \\ x_i y_i \geq \alpha_{i^*} \beta_{i^*}}} d(\alpha_i, x_i) + d(\beta_i, y_i)} \quad (6) \\ &\stackrel{(i)}{\leq} \underbrace{\sum_{i \neq i^*} \frac{\Delta_i}{\min_{\substack{0 \leq x_i, y_i \leq 1 \\ x_i y_i \geq \alpha_{i^*} \beta_{i^*}}} d(\alpha_i, x_i) + d(\beta_i, y_i)}}_{\text{2/B/B lower bound constant derived by [4]}} \\ &\stackrel{(ii)}{\leq} \underbrace{\sum_{i \neq i^*} \frac{\Delta_i}{\min_{\substack{0 \leq x_i, y_i \leq 1 \\ x_i y_i \geq \alpha_{i^*} \beta_{i^*}}} d(\alpha_i \beta_i, x_i y_i)}}_{\text{1/B lower bound constant derived by [22]}} \end{aligned}$$

The above shows that the lower bound constant under 2/F/B given in Theorem 1 is smaller than the lower bound constant under 2/B/B derived by Gupta et al. [4]. This follows from the relationship (i), which shows the lower bound constant under 2/B/B minimizes the denominator for the suboptimal arms satisfying $\alpha_i > \alpha_{i^*} \beta_{i^*}$, unlike the lower bound constant under 2/F/B. The relationship (ii) between the lower bound constants under 2/B/B feedback and 1/B feedback is proven in Theorem 2 of [4].

We further illustrate the size comparison between the lower bound constants under 2/F/B, 2/B/B, and 1/B feedback shown in Remark 1 by numerical simulations with two arms. Specially, we set the optimal arm’s prediction and transmission rates as $\alpha_{i^*} = 0.8$ and $\beta_{i^*} = 0.9$, respectively. In the first example (Figure 2a), we fix the suboptimal arm’s transmission rate at 0.8 and vary its prediction rate across the set $[0.75, 0.8, 0.85, 0.9]$. In the second example (Figure 2b), we fix the prediction rate at 0.75 and vary the transmission rate across $[0.6, 0.7, 0.8, 0.9]$. In Figure 2, we observe that the lower bound constants corresponding to 1/B and 2/B/B settings exhibit small differences. In contrast, the lower bound constant of 2/F/B is significantly smaller, indicating that a learning algorithm may substantially reduce its regret by exploiting the additional full-information feedback.

B. Regret Upper Bound of AdaPort

In the following theorem, we validate that AdaPort (Algorithm 1) achieves an upper bound constant equal to the lower bound constant in Theorem 1, demonstrating its asymptotic optimality.

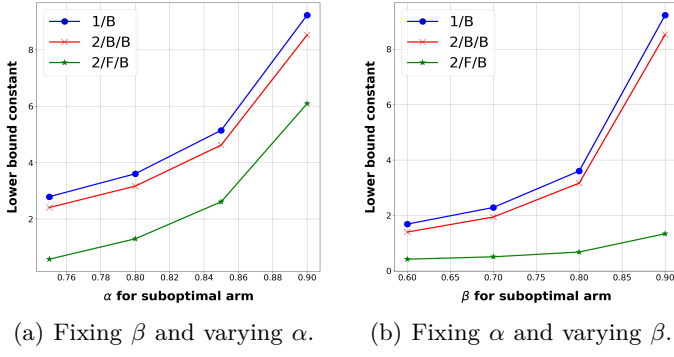


Fig. 2: Lower bound constant comparison for two arms.

Theorem 2. (Upper bound) AdaPort (Algorithm 1) achieves an asymptotic regret upper bound of

$$\limsup_{T \rightarrow \infty} \frac{R(T)}{\log T} \leq \sum_{i \neq i^* : \alpha_i > \alpha_{i^*} \beta_{i^*}} \frac{\Delta_i}{d\left(\beta_i, \frac{\alpha_{i^*} \beta_{i^*}}{\alpha_i}\right)}. \quad (7)$$

Proof. Recall from (1) that the regret can be decomposed as $R(T) = \sum_{i \neq i^*} \Delta_i \mathbb{E}[n_i(T)]$. Fix an arbitrary suboptimal arm $i \neq i^*$. Then it suffices to show that

$$\limsup_{T \rightarrow \infty} \frac{\mathbb{E}[n_i(T)]}{\log T} \leq \begin{cases} \frac{1}{d(\beta_i, \frac{\alpha_{i^*} \beta_{i^*}}{\alpha_i})} & \alpha_i > \alpha_{i^*} \beta_{i^*} \\ 0 & \alpha_i \leq \alpha_{i^*} \beta_{i^*} \end{cases}. \quad (8)$$

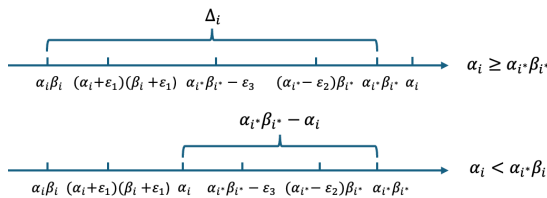
We begin by selecting $\epsilon_1, \epsilon_2, \epsilon_3 > 0$ that satisfy

$$(\alpha_i + \epsilon_1)(\beta_i + \epsilon_1) < \alpha_{i^*} \beta_{i^*} - \epsilon_3 < (\alpha_{i^*} - \epsilon_2)\beta_{i^*}, \quad (9)$$

where the first inequality is applied in deriving (12), while the second inequality is applied in deriving (11).

In particular, fix $\epsilon_3 \in (0, \epsilon_3^{\max})$ where

$$\epsilon_3^{\max} \triangleq \begin{cases} \Delta_i & \alpha_i \geq \alpha_{i^*} \beta_{i^*} \\ \alpha_{i^*} \beta_{i^*} - \alpha_i & \alpha_i < \alpha_{i^*} \beta_{i^*} \end{cases}.$$

Fig. 3: The range of ϵ_3 .

Then define the intervals $\Gamma_1 \triangleq (0, \epsilon_1^{\max})$ and $\Gamma_2 \triangleq \left(0, \frac{\epsilon_3}{\beta_{i^*}}\right)$ where $\epsilon_1^{\max} \triangleq \frac{\sqrt{(\alpha_i + \beta_i)^2 + 4(\Delta_i - \epsilon_3)} - (\alpha_i + \beta_i)}{2}$ and fix $\epsilon_1 \in \Gamma_1$ and $\epsilon_2 \in \Gamma_2$. Note that ϵ_1^{\max} is a zero of the quadratic function $q_i(\epsilon_1) = \epsilon_1^2 + (\alpha_i + \beta_i)\epsilon_1 - (\Delta_i - \epsilon_3)$. Then since $\epsilon_1 < \epsilon_1^{\max}$, we have $q_i(\epsilon_1) < 0$ due to the convexity of $q_i(\epsilon_1)$. Rearranging gives $\epsilon_1^2 + (\alpha_i + \beta_i)\epsilon_1 < \Delta_i - \epsilon_3$, and adding $\alpha_i \beta_i$ to both sides and factoring the left-hand side gives $(\alpha_i + \epsilon_1)(\beta_i + \epsilon_1) < \alpha_{i^*} \beta_{i^*} - \epsilon_3$. Combining this lower bound with the upper bound $\alpha_{i^*} \beta_{i^*} - \epsilon_3 < (\alpha_{i^*} - \epsilon_2)\beta_{i^*}$,

which follows directly from the definition of Γ_2 and the fact that $\epsilon_2 \in \Gamma_2$, gives the desired (9).

Next, we use $\epsilon_1, \epsilon_2, \epsilon_3$ to define the following three events, which will be used to decompose $\mathbb{E}[n_i(T)]$:

Definition 1. (Events $E_i^\mu(t)$, $E_{i^*}^\mu(t)$, and $E_i^\theta(t)$)

For each time step t , we define the following events:

$$1) E_i^\mu(t) \triangleq \{|\bar{\alpha}_i(t) - \alpha_i| \leq \epsilon_1, |\bar{\beta}_i(t) - \beta_i| \leq \epsilon_1\}, \text{ where}$$

$$\bar{\beta}_i(t) = \begin{cases} \frac{1}{n_i(t-1)} \sum_{s=1}^{n_i(t-1)} Y_i(\tau_{s,i}), & \text{if } n_i(t-1) > 0 \\ 0, & \text{otherwise} \end{cases},$$

and $\tau_{s,i}$ denotes the timeslot that the fixed suboptimal arm i was played for the s -th time.

$$2) E_{i^*}^\mu(t) \triangleq \{|\bar{\alpha}_{i^*}(t) - \alpha_{i^*}| \leq \epsilon_2\}.$$

$$3) E_i^\theta(t) \triangleq \{\bar{\alpha}_i(t) \theta_{\beta,i}(t) \leq \alpha_{i^*} \beta_{i^*} - \epsilon_3\}.$$

Consider the following four events composed from the events from Definition 1:

$$(i) \{i(t) = i\} \cap E_i^\mu(t) \cap E_i^\theta(t) \cap E_{i^*}^\mu(t),$$

$$(ii) \{i(t) = i\} \cap E_i^\mu(t) \cap E_i^\theta(t) \cap \overline{E_{i^*}^\mu(t)},$$

$$(iii) \{i(t) = i\} \cap E_i^\mu(t) \cap \overline{E_i^\theta(t)}, \text{ and}$$

$$(iv) \{i(t) = i\} \cap \overline{E_i^\mu(t)}.$$

These events are mutually exclusive and collectively exhaustive, and moreover, for event (ii), we have $\{i(t) = i\} \cap E_i^\mu(t) \cap E_i^\theta(t) \cap \overline{E_{i^*}^\mu(t)} \subseteq \overline{E_{i^*}^\mu(t)}$. By the monotonicity of probability and the law of total probability, we therefore bound

$$\begin{aligned} \mathbb{E}[n_i(T)] &= \sum_{t=1}^T \Pr(i(t) = i) \\ &\leq \sum_{t=1}^T \Pr(i(t) = i, E_i^\mu(t), E_i^\theta(t), E_{i^*}^\mu(t)) \\ &\quad + \sum_{t=1}^T \Pr(\overline{E_{i^*}^\mu(t)}) \\ &\quad + \sum_{t=1}^T \Pr(i(t) = i, E_i^\mu(t), \overline{E_i^\theta(t)}) \\ &\quad + \sum_{t=1}^T \Pr(i(t) = i, \overline{E_i^\mu(t)}). \end{aligned} \quad (10)$$

The following lemma, whose proof can be found in Appendix B and relies on the relationship (9) between $\epsilon_1, \epsilon_2, \epsilon_3$, bounds each of the terms above:

Lemma 1. Each of the terms in (10) can be bounded by

$$\sum_{t=1}^T \Pr(i(t) = i, E_i^\mu(t), E_i^\theta(t), E_{i^*}^\mu(t)) \leq M_1, \quad (11)$$

$$\begin{aligned} \sum_{t=1}^T \Pr(i(t) = i, E_i^\mu(t), \overline{E_i^\theta(t)}) \\ \leq \begin{cases} \inf_{\epsilon_1 \in \Gamma_1} \frac{\log T}{d(\beta_i + \epsilon_1, \frac{\alpha_{i^*} \beta_{i^*} - \epsilon_3}{\alpha_i + \epsilon_1})} + 1 & \alpha_i \geq \alpha_{i^*} \beta_{i^*} \\ M_2 & \alpha_i < \alpha_{i^*} \beta_{i^*} \end{cases}, \end{aligned} \quad (12)$$

$$\sum_{t=1}^T \Pr(i(t) = i, \overline{E_i^\mu(t)}) \leq M_3, \quad (13)$$

$$\sum_{t=1}^T \Pr(\overline{E_{i^*}^\mu(t)}) \leq M_4, \quad (14)$$

where $M_1 \triangleq \inf_{\epsilon_2 \in \Gamma_2} \left(\frac{24}{\Delta'^2} + \Theta\left(\frac{1}{\Delta'^2} + \frac{1}{\Delta'^2 D} + \frac{1}{\Delta'^4}\right) \right)$, $\Delta' = \beta_{i^*} - x$, $D \triangleq d(x, \beta_{i^*}) = x \log \frac{x}{\beta_{i^*}} + (1-x) \log \frac{1-x}{1-\beta_{i^*}}$, $x \triangleq \frac{\alpha_{i^*} \beta_{i^*} - \epsilon_3}{\alpha_{i^*} - \epsilon_2}$, $M_2 \triangleq \inf_{\epsilon_4 \in \Gamma_4} \frac{1}{2\epsilon_4^2} + 1$, $\Gamma_4 \triangleq$

$$(0, \max\{0, \alpha_{i^*}\beta_{i^*} - \alpha_i - \epsilon_3\}), M_3 \triangleq \inf_{\epsilon_1 \in \Gamma_1} \frac{2}{\epsilon_1^2} + 1, M_4 \triangleq \inf_{\epsilon_2 \in \Gamma_2} \frac{1}{\epsilon_2^2} + 1.$$

From (10) and Lemma 1, it follows that if $\alpha_i < \alpha_{i^*}\beta_{i^*}$, then

$$\mathbb{E}[n_i(T)] \leq M_1 + M_2 + M_3 + M_4. \quad (15)$$

In this case, since M_1, M_2, M_3, M_4 are constants, it follows that $\limsup_{T \rightarrow \infty} \frac{\mathbb{E}[n_i(T)]}{\log T} = 0$, which agrees with (8). On the other hand, if $\alpha_i \geq \alpha_{i^*}\beta_{i^*}$, then (10) and Lemma 1 give that

$$\mathbb{E}[n_i(T)] \leq \inf_{\epsilon_1 \in \Gamma_1} \frac{\log T}{d\left(\beta_i + \epsilon_1, \frac{\alpha_{i^*}\beta_{i^*} - \epsilon_3}{\alpha_i + \epsilon_1}\right)} + M_1 + M_3 + M_4 + 1, \quad (16)$$

and therefore

$$\begin{aligned} \limsup_{T \rightarrow \infty} \frac{\mathbb{E}[n_i(T)]}{\log T} &= \inf_{\epsilon_1 \in \Gamma_1} \frac{1}{d\left(\beta_i + \epsilon_1, \frac{\alpha_{i^*}\beta_{i^*} - \epsilon_3}{\alpha_i + \epsilon_1}\right)} \\ &= \frac{1}{d\left(\beta_i, \frac{\alpha_{i^*}\beta_{i^*} - \epsilon_3}{\alpha_i}\right)}. \end{aligned} \quad (17)$$

Since ϵ_3 can be taken arbitrarily small and positive, we conclude that $\limsup_{T \rightarrow \infty} \frac{\mathbb{E}[n_i(T)]}{\log T} \leq \frac{1}{d\left(\beta_i, \frac{\alpha_{i^*}\beta_{i^*}}{\alpha_i}\right)}$, which agrees with (8). \square

Remark 2. According to Lemma 1, the regret contribution from $\sum_{t=1}^T \Pr\left(i(t) = i, E_i^\mu(t), E_i^\theta(t)\right)$ is of order $O(\log T)$. Under the 2/B/B feedback model, even if the empirical estimates $\bar{\alpha}_i(t)$ and $\bar{\beta}_i(t)$ are close to their true means α_i and β_i , the arm selection remains uncertain due to the stochasticity of both $\theta_{\alpha,i}(t)$ and $\theta_{\beta,i}(t)$. These variables represent Thompson Sampling draws for the transmission and prediction rates, respectively, and are updated based on bandit feedback [4], [5]. Thus, uncertainty persists in both dimensions. In contrast, under the 2/F/B feedback model, the transmission rate α_i is estimated with full information, so $\bar{\alpha}_i(t)$ concentrates rapidly around α_i . As a result, the only remaining source of exploration-induced randomness is $\theta_{\beta,i}(t)$, which governs the uncertainty in the transmission rate. This reduction in uncertainty leads to more confident decision-making and lower regret in practice.

VI. Empirical Evaluation

In this section, we evaluate our theoretical regret upper bound in real-world trace-based simulations using data traces collected from a user interacting with a panoramic video stream and measured wireless bandwidth. We compare the performance of our algorithm against three baseline algorithms:

- 1) Thompson sampling under 1/B feedback (1/B-TS): the standard Thompson sampling MAB algorithm.
- 2) Thompson sampling under 2/B/B feedback (2/B/B-TS): two-level Thompson sampling (Chen et al. [5]).
- 3) EXP3 under 1/B feedback (1/B-EXP3): an optimal algorithm for adversarial bandits (Auer et al. [24]).

4) Heuristic minimum scene delivery (Heuristic): a heuristic method based on the Flare system [8] that delivers only those tiles overlapping with the user's predicted viewport.

(2) is state-of-the-art algorithms for the portion selection problem, while (3) is chosen to test our i.i.d. prediction and transmission assumptions. In the following subsections, we detail our findings for the trace-based simulations. In order to evaluate user experience, we also plot the relative throughput degradation compared to the optimal policy, which is given by:

$$\mathbb{E}\left[\frac{\sum_{t=1}^T (1 - Z_{i(t)}(t)) - \sum_{t=1}^T (1 - Z_{i^*}(t))}{\sum_{t=1}^T (1 - Z_{i^*}(t))}\right]. \quad (18)$$

In the following, we present a detailed characterization of the real-world data traces used in our evaluation:

1) **Delivery portions:** We collect a data trace from a user viewing a free educational panoramic video (see [25]). The trace captures a 3 DoF (orientation only) head motion over 3000 timeslots. We iterate over the dataset multiple times to achieve a total of $T = 3 \times 10^4$ timeslots for our experiments. At each timeslot t , we apply a linear regression model to the motion trace in order to predict the user's head pose for the subsequent timeslot $t + 1$. The model is trained using motion trajectories from the preceding three timeslots. We set $N = 4$ different portions to select from: $100^\circ \times 90^\circ$ (minimum viewport), $102^\circ \times 91^\circ$, $108^\circ \times 94^\circ$, and $120^\circ \times 100^\circ$, where each pair gives the angles corresponding to the yaw and pitch axes, respectively. For each portion $i \in [N]$, we compute $X_i(t)$ from the user's actual head pose (received in the ACK packet) and the server's predicted head pose, as described in step (4) in Section III.

2) **Wireless Transmissions:** We collected wireless bandwidth traces using iPerf2 in reverse UDP mode with a reporting interval of 10 ms (corresponding to 100 FPS). In this configuration, the server transmits UDP probe packets at a fixed sending rate, allowing the client to measure the instantaneous downlink throughput. These traces capture the short-term variability of the wireless channel under target sending rates of 100 Mbps and 150 Mbps. To ensure that the measured throughput accurately reflects the underlying available bandwidth (channel capacity) rather than server-side fluctuations, we maintain a constant sending rate throughout the trace collection. For each interval, the transmission delay of a data portion is calculated as the ratio of its size to the measured bandwidth. A portion is considered successfully delivered if its transmission delay does not exceed the interval duration.

3) **Comparison with heuristic minimum scene delivery:** Figure 4 compares the relative throughput degradation of the heuristic minimum scene delivery against various Thompson Sampling-based approaches. As illustrated in Figure 4(a), the heuristic achieves the lowest degradation in the 100 Mbps sending rate regime, surpassing

all Thompson Sampling-based methods. However, as the sending rate increases, shown in Figure 4(b), the heuristic's performance deteriorates substantially, with degradation escalating to 16.1%. Conversely, AdaPort demonstrates superior performance near the optimal throughput. This divergence further justifies the requirement for adaptive learning mechanisms to handle dynamic network conditions.

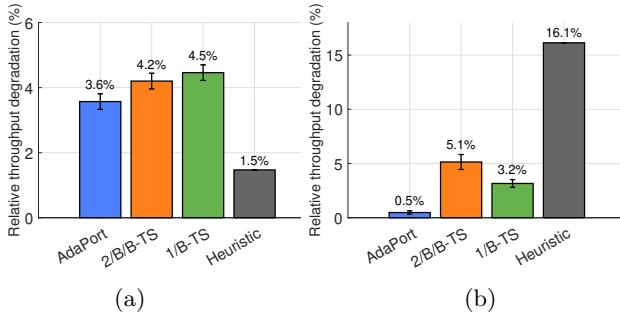


Fig. 4: Trace-based simulations: AdaPort compared against Thompson sampling under 2/B/B and 1/B feedback. (a) and (b) show the relative throughput degradation compared to the optimal policy using fixed sending rates at 100 Mbps and 150 Mbps, respectively.

4) Comparison with 1/B-TS and 2/B/B-TS: As illustrated in Figure 4, AdaPort consistently outperforms both 1/B-TS and 2/B/B-TS, with the performance gap becoming particularly pronounced at a sending rate of 150 Mbps as shown in Fig. 4b. Under this setting, the observed transmission success rates for all portions fall within a narrow range of approximately 0.97–0.99. This observation is consistent with our intuition: when network conditions are highly reliable, transmission randomness becomes negligible, and prediction uncertainty emerges as the dominant source of variability. By leveraging richer prediction feedback, AdaPort effectively reduces this uncertainty, thereby achieving superior performance. Consequently, under high-quality and stable network environments, AdaPort delivers performance that surpasses state-of-the-art baselines. Notably, AdaPort incurs less than a 4% increase in failed deliveries during learning, yielding a near-optimal user experience at a 100 Mbps sending rate and achieving almost optimal performance at 150 Mbps.

In addition, when considered alongside the theoretical lower-bound results in Figure 2, we observe that incorporating additional bandit feedback may produce only marginal improvements in regret. Empirically, this trend is further manifested in the sending rate as 150 Mbps, where 2/B/B-TS performs worse than 1/B-TS, suggesting that additional feedback does not necessarily translate into improved performance in practical settings.

5) Comparison with 1/B-TS and 1/B-EXP3: Recall that our i.i.d. assumptions about the prediction and transmission outcomes in Section III may not be realistic in practice. Therefore, we compare AdaPort, as well as

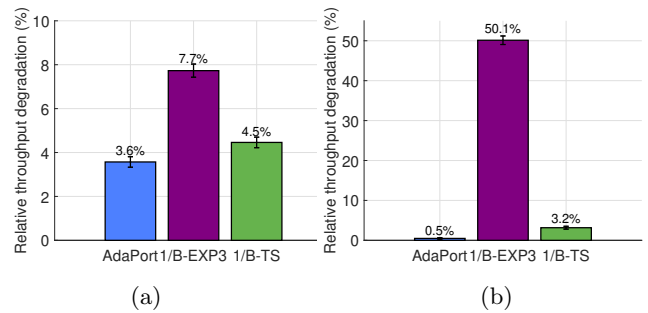


Fig. 5: Trace-based simulations: AdaPort compared against Thompson sampling and EXP3 under 1/B feedback. (a) and (b) show the relative throughput degradation compared to the optimal policy using fixed sending rates at 100 Mbps and 150 Mbps, respectively.

1/B-TS against 1/B-EXP3, which is a well-established algorithm designed for adversarial multi-armed bandit scenarios. As illustrated in Figure 5, both AdaPort and 1/B-TS outperform 1/B-EXP3, indicating that our algorithm remains effective even when applied to non-i.i.d. real-world data traces.

VII. Conclusion and future work

In this paper, we investigated a hybrid feedback-driven online learning framework tailored to the interactive delivery of panoramic scenes over wireless networks. A critical observation is that, upon receiving the user's current head movement data, the system can determine whether each candidate portion successfully covers the user's viewport. This implies that the prediction feedback can be categorized as full-information feedback. We first establish a theoretical improvement in the regret lower bound for 2/F/B, as compared to 2/B/B and 1/B feedback. This highlights the potential benefit of leveraging full-information predictions to enhance regret performance. Building on this, we propose AdaPort, a hybrid learning algorithm that leverages both the full-information feedback and bandit feedback and demonstrate that the proposed algorithm is asymptotically optimal. Real-world trace-based experiments validate the superior performance of our approach relative to state-of-the-art portion selection algorithms. In future work, we plan to investigate more realistic reward models that better capture the nuances of user experience. For example, we aim to refine the definition of delivery success by accounting for cases in which only a small portion of a segment fails to be delivered. Such partial failures may have minimal impact on the user's viewing experience and thus should not necessarily be treated as complete delivery failures. We also intend to explore alternative problem formulations, such as nonstationary bandits, to more accurately reflect the dynamics of real-world panoramic scene delivery.

References

[1] Y. Bao, H. Wu, T. Zhang, A. A. Ramli, and X. Liu, "Shooting a moving target: Motion-prediction-based transmission for 360-degree videos," in 2016 IEEE International Conference on Big Data (Big Data), 2016, pp. 1161–1170.

[2] "Meta horizon - testing and performance analysis." [Online]. Available: <https://developers.meta.com/horizon/documentation/unity/unity-perf/>

[3] J. Wang, R. Shi, W. Zheng, W. Xie, D. Kao, and H.-N. Liang, "Effect of frame rate on user experience, performance, and simulator sickness in virtual reality," *IEEE Transactions on Visualization and Computer Graphics*, vol. 29, no. 5, pp. 2478–2488, 2023.

[4] H. Gupta, J. Chen, B. Li, and R. Srikant, "Online learning-based rate selection for wireless interactive panoramic scene delivery," in IEEE INFOCOM 2022-IEEE Conference on Computer Communications. IEEE, 2022, pp. 1799–1808.

[5] J. Chen, B. Li, and R. Srikant, "Thompson-sampling-based wireless transmission for panoramic video streaming," in 2020 18th International Symposium on Modeling and Optimization in Mobile, Ad Hoc, and Wireless Networks (WiOPT). IEEE, 2020, pp. 1–3.

[6] X. Wu, J. Steiger, B. Li, and R. Srikant, "Optimal hybrid feedback-driven learning for wireless interactive panoramic scene delivery," in Proceedings of the Twenty-sixth International Symposium on Theory, Algorithmic Foundations, and Protocol Design for Mobile Networks and Mobile Computing, 2025, pp. 341–350.

[7] X. Liu, C. Vlachou, M. Yang, F. Qian, L. Zhou, C. Wang, L. Zhu, K.-H. Kim, G. Parmer, Q. Chen et al., "Firefly: Untethered multi-user {VR} for commodity mobile devices," in 2020 USENIX Annual Technical Conference (USENIX ATC 20), 2020, pp. 943–957.

[8] F. Qian, B. Han, Q. Xiao, and V. Gopalakrishnan, "Flare: Practical viewport-adaptive 360-degree video streaming for mobile devices," in Proceedings of the 24th Annual International Conference on Mobile Computing and Networking, 2018, pp. 99–114.

[9] J. Chakareski, "Viewport-adaptive scalable multi-user virtual reality mobile-edge streaming," *IEEE Transactions on Image Processing*, vol. 29, pp. 6330–6342, 2020.

[10] J. Chen, X. Qin, G. Zhu, B. Ji, and B. Li, "Motion-prediction-based wireless scheduling for multi-user panoramic video streaming," in IEEE INFOCOM 2021-IEEE Conference on Computer Communications. IEEE, 2021, pp. 1–10.

[11] X. Wu and B. Li, "Achieving regular and fair learning in combinatorial multi-armed bandit," in IEEE INFOCOM 2024 - IEEE Conference on Computer Communications, 2024, pp. 361–370.

[12] J. Steiger, X. Wu, and B. Li, "Learning to wirelessly deliver consistent and high-quality interactive panoramic scenes," in 2025 23st International Symposium on Modeling and Optimization in Mobile, Ad Hoc, and Wireless Networks (WiOpt). IEEE, 2025.

[13] P. Auer, N. Cesa-Bianchi, and P. Fischer, "Finite-time analysis of the multiarmed bandit problem," *Machine learning*, vol. 47, pp. 235–256, 2002.

[14] A. Garivier and O. Cappé, "The kl-ucb algorithm for bounded stochastic bandits and beyond," in Proceedings of the 24th annual conference on learning theory. JMLR Workshop and Conference Proceedings, 2011, pp. 359–376.

[15] S. Agrawal and N. Goyal, "Near-optimal regret bounds for thompson sampling," *Journal of the ACM (JACM)*, vol. 64, no. 5, pp. 1–24, 2017.

[16] H. Zhao and W. Chen, "Stochastic one-sided full-information bandit," in Joint European Conference on Machine Learning and Knowledge Discovery in Databases. Springer, 2019, pp. 150–166.

[17] N. Alon, N. Cesa-Bianchi, C. Gentile, S. Mannor, Y. Mansour, and O. Shamir, "Nonstochastic multi-armed bandits with graph-structured feedback," *SIAM Journal on Computing*, vol. 46, no. 6, pp. 1785–1826, 2017.

[18] Y.-H. Yan, P. Zhao, and Z.-H. Zhou, "Online non-stochastic control with partial feedback," *Journal of Machine Learning Research*, vol. 24, no. 273, pp. 1–50, 2023.

[19] Q. Zhang, Z. Deng, Z. Chen, K. Zhou, H. Hu, and Y. Yang, "Online learning for non-monotone dr-submodular maximization: From full information to bandit feedback," in International Conference on Artificial Intelligence and Statistics. PMLR, 2023, pp. 3515–3537.

[20] F. Liu, S. Buccapatnam, and N. Shroff, "Information directed sampling for stochastic bandits with graph feedback," in Proceedings of the AAAI Conference on Artificial Intelligence, vol. 32, no. 1, 2018.

[21] D. Cheng, X. Zhou, and B. Ji, "Understanding the role of feedback in online learning with switching costs," 2023. [Online]. Available: <https://arxiv.org/abs/2306.09588>

[22] T. L. Lai and H. Robbins, "Asymptotically efficient adaptive allocation rules," *Advances in applied mathematics*, vol. 6, no. 1, pp. 4–22, 1985.

[23] T. Lattimore and C. Szepesvári, *Bandit algorithms*. Cambridge University Press, 2020.

[24] P. Auer, N. Cesa-Bianchi, Y. Freund, and R. E. Schapire, "The nonstochastic multiarmed bandit problem," *SIAM journal on computing*, vol. 32, no. 1, pp. 48–77, 2002.

[25] N. Geographic, "First-ever 3d vr filmed in space." [Online]. Available: <https://vuzel.camera/vr-gallery/3d-360-video/first-ever-3d-vr-filmed-space>

Appendix A
Proof of Theorem 1

To prove Theorem 1, we require the following divergence decomposition lemma, which can be thought of as a version of Lemma 15.1 in [23] for 2/F/B feedback.

Lemma 2. Consider an alternative set of system parameters (α', β') , and the corresponding probability measure Pr' under these parameters. Let (π) be an arbitrary randomized policy that learns from 2/F/B feedback and let p_π and p'_π denote the probability mass functions of the sequence of observations $(i(t), \mathbf{X}(t), Y_{i(t)}(t))_{t=1}^T$ when the policy (π) is used under the probability measures Pr and Pr' respectively. Then

$$D_{\text{KL}}(p_\pi \parallel p'_\pi) = TD_{\text{KL}}(p_{\mathbf{X}} \parallel p'_{\mathbf{X}}) + \sum_{i=1}^N D_{\text{KL}}(p_{Y_i} \parallel p'_{Y_i}) \sum_{t=1}^T \text{Pr}(i(t) = i) \quad (19)$$

where $p_{\mathbf{X}}(\mathbf{x}) \triangleq \text{Pr}(\mathbf{X}(1) = \mathbf{x})$, $p'_{\mathbf{X}}(\mathbf{x}) \triangleq \text{Pr}'(\mathbf{X}(1) = \mathbf{x})$, $p_{Y_i}(y_i) \triangleq \text{Pr}(Y_i(1) = y_i)$, and $p'_{Y_i}(y_i) \triangleq \text{Pr}'(Y_i(1) = y_i)$.

Proof. For convenience, let $\mathbf{W}_t \triangleq (i(t), \mathbf{X}(t), Y_{i(t)}(t))$ denote the vector of observations from timeslot t . Fix an arbitrary randomized policy (π) specified by a probability mass function $\pi_t(\cdot \mid \mathbf{w}_{1:t-1}) : [N] \rightarrow [0, 1]$ for each timeslot t and possible trajectory of prior observations $\mathbf{w}_{1:t-1} \in \text{support}(\mathbf{W}_{1:t-1})$. The policy therefore plays the arm $i(t) \sim \pi_t(\cdot \mid \mathbf{W}_{1:t-1})$ in each timeslot t .

By the chain rule of probability, we have

$$\text{Pr}(\mathbf{W}_{1:T} = \mathbf{w}_{1:T}) = \prod_{t=1}^T \text{Pr}(\mathbf{W}_t = \mathbf{w}_t \mid \mathbf{W}_{1:t-1} = \mathbf{w}_{1:t-1}) \quad (20)$$

(taking the event $\{\mathbf{W}_{1:t-1} = \mathbf{w}_{1:t-1}\}$ when $t = 1$ to be equal to the sample space for notational convenience). Similarly,

$$\Pr'(\mathbf{W}_{1:T} = \mathbf{w}_{1:T}) = \prod_{t=1}^T \Pr'(\mathbf{W}_t = \mathbf{w}_t \mid \mathbf{W}_{1:t-1} = \mathbf{w}_{1:t-1}). \quad (21)$$

For each timeslot t , define the function

$$f_t(\mathbf{w}_{1:t}) \triangleq \log \frac{\Pr(\mathbf{W}_t = \mathbf{w}_t \mid \mathbf{W}_{1:t-1} = \mathbf{w}_{1:t-1})}{\Pr'(\mathbf{W}_t = \mathbf{w}_t \mid \mathbf{W}_{1:t-1} = \mathbf{w}_{1:t-1})}. \quad (22)$$

Then it follows from (20) and (21) that

$$\log \frac{\Pr(\mathbf{W}_{1:T} = \mathbf{w}_{1:T})}{\Pr'(\mathbf{W}_{1:T} = \mathbf{w}_{1:T})} = \sum_{t=1}^T f_t(\mathbf{w}_{1:t}). \quad (23)$$

Then we have

$$\begin{aligned} D_{\text{KL}}(p_{\pi} \parallel p'_{\pi}) &= \sum_{\mathbf{w}_{1:T}} \Pr(\mathbf{W}_{1:T} = \mathbf{w}_{1:T}) \log \frac{\Pr(\mathbf{W}_{1:T} = \mathbf{w}_{1:T})}{\Pr'(\mathbf{W}_{1:T} = \mathbf{w}_{1:T})} \\ &= \sum_{\mathbf{w}_{1:T}} \Pr(\mathbf{W}_{1:T} = \mathbf{w}_{1:T}) \sum_{t=1}^T f_t(\mathbf{w}_{1:t}) \\ &\stackrel{(a)}{=} \mathbb{E} \left[\sum_{t=1}^T f_t(\mathbf{W}_{1:t}) \right] = \sum_{t=1}^T \mathbb{E}[f_t(\mathbf{W}_{1:t})] \\ &= \sum_{t=1}^T \sum_{\mathbf{w}_{1:t}} \Pr(\mathbf{W}_{1:t} = \mathbf{w}_{1:t}) f_t(\mathbf{w}_{1:t}) \end{aligned} \quad (24)$$

where (a) is by the law of the unconscious statistician. Fix a timeslot t and a sample path $\mathbf{w}_{1:t}$ such that $\mathbf{w}_t = (i, \mathbf{x}, y_i)$. Then

$$\begin{aligned} f_t(\mathbf{w}_{1:t}) &= \log \frac{\Pr(\mathbf{W}_t = (i, \mathbf{x}, y_i) \mid \mathbf{W}_{1:t-1} = \mathbf{w}_{1:t-1})}{\Pr'(\mathbf{W}_t = (i, \mathbf{x}, y_i) \mid \mathbf{W}_{1:t-1} = \mathbf{w}_{1:t-1})} \\ &= \log \frac{\Pr(i(t) = i, \mathbf{X}(t) = \mathbf{x}, Y_i(t) = y_i \mid \mathbf{W}_{1:t-1} = \mathbf{w}_{1:t-1})}{\Pr'(i(t) = i, \mathbf{X}(t) = \mathbf{x}, Y_i(t) = y_i \mid \mathbf{W}_{1:t-1} = \mathbf{w}_{1:t-1})} \\ &\stackrel{(a)}{=} \log \frac{\Pr(i(t) = i \mid \mathbf{W}_{1:t-1} = \mathbf{w}_{1:t-1}) p_{\mathbf{X}}(\mathbf{x}) p_{Y_i}(y_i)}{\Pr'(i(t) = i \mid \mathbf{W}_{1:t-1} = \mathbf{w}_{1:t-1}) p'_{\mathbf{X}}(\mathbf{x}) p'_{Y_i}(y_i)} \\ &\stackrel{(b)}{=} \log \frac{\pi_t(i \mid \mathbf{w}_{1:t-1}) p_{\mathbf{X}}(\mathbf{x}) p_{Y_i}(y_i)}{\pi_t(i \mid \mathbf{w}_{1:t-1}) p'_{\mathbf{X}}(\mathbf{x}) p'_{Y_i}(y_i)} = \log \frac{p_{\mathbf{X}}(\mathbf{x}) p_{Y_i}(y_i)}{p'_{\mathbf{X}}(\mathbf{x}) p'_{Y_i}(y_i)} \end{aligned} \quad (25)$$

where (a) is because $\mathbf{X}(t)$ and $Y_i(t)$ are independent and both i.i.d. over time, and therefore are independent from the history $\mathbf{W}_{1:t-1}$ and decision $i(t)$, and (b) is because only the parameters $(\boldsymbol{\alpha}, \boldsymbol{\beta})$ change to $(\boldsymbol{\alpha}', \boldsymbol{\beta}')$ between the probability measures Pr and Pr' and therefore the additional randomness introduced by the randomized policy is distributed the same under both probability

measures. It follows from (24) that

$$\begin{aligned} D_{\text{KL}}(p_{\pi} \parallel p'_{\pi}) &= \sum_{t=1}^T \sum_{\mathbf{w}_{1:t}} \Pr(\mathbf{W}_{1:t} = \mathbf{w}_{1:t}) f_t(\mathbf{w}_{1:t}) \\ &= \sum_{t=1}^T \sum_{(i, \mathbf{x}, y_i)} \sum_{\mathbf{w}_{1:t} : \mathbf{w}_t = (i, \mathbf{x}, y_i)} \Pr(\mathbf{W}_{1:t} = \mathbf{w}_{1:t}) f_t(\mathbf{w}_{1:t}) \\ &\stackrel{(a)}{=} \sum_{t=1}^T \sum_{(i, \mathbf{x}, y_i)} \sum_{\mathbf{w}_{1:t} : \mathbf{w}_t = (i, \mathbf{x}, y_i)} \Pr(\mathbf{W}_{1:t} = \mathbf{w}_{1:t}) \log \frac{p_{\mathbf{X}}(\mathbf{x}) p_{Y_i}(y_i)}{p'_{\mathbf{X}}(\mathbf{x}) p'_{Y_i}(y_i)} \\ &= \sum_{t=1}^T \sum_{(i, \mathbf{x}, y_i)} \log \frac{p_{\mathbf{X}}(\mathbf{x}) p_{Y_i}(y_i)}{p'_{\mathbf{X}}(\mathbf{x}) p'_{Y_i}(y_i)} \sum_{\mathbf{w}_{1:t} : \mathbf{w}_t = (i, \mathbf{x}, y_i)} \Pr(\mathbf{W}_{1:t} = \mathbf{w}_{1:t}) \\ &\stackrel{(b)}{=} \sum_{t=1}^T \sum_{(i, \mathbf{x}, y_i)} \log \frac{p_{\mathbf{X}}(\mathbf{x}) p_{Y_i}(y_i)}{p'_{\mathbf{X}}(\mathbf{x}) p'_{Y_i}(y_i)} \Pr(\mathbf{W}_t = (i, \mathbf{x}, y_i)) \end{aligned} \quad (26)$$

where (a) is from (25) and (b) applies the law of total probability. Since $i(t)$, $\mathbf{X}(t)$, and $Y_i(t)$ are independent, for each timeslot t and observation vector (i, \mathbf{x}, y_i) , we have

$$\begin{aligned} \Pr(\mathbf{W}_t = (i, \mathbf{x}, y_i)) &= \Pr(i(t) = i, \mathbf{X}(t) = \mathbf{x}, Y_i(t) = y_i) \\ &= \Pr(i(t) = i) p_{\mathbf{X}}(\mathbf{x}) p_{Y_i}(y_i). \end{aligned} \quad (27)$$

Plugging the above into (26) gives

$$\begin{aligned} D_{\text{KL}}(p_{\pi} \parallel p'_{\pi}) &= \sum_{t=1}^T \sum_{(i, \mathbf{x}, y_i)} \log \frac{p_{\mathbf{X}}(\mathbf{x}) p_{Y_i}(y_i)}{p'_{\mathbf{X}}(\mathbf{x}) p'_{Y_i}(y_i)} \Pr(i(t) = i) p_{\mathbf{X}}(\mathbf{x}) p_{Y_i}(y_i) \\ &= \sum_{t=1}^T \underbrace{\sum_{i=1}^N \Pr(i(t) = i)}_{=1} \underbrace{\sum_{\mathbf{x}} p_{\mathbf{X}}(\mathbf{x}) \log \frac{p_{\mathbf{X}}(\mathbf{x})}{p'_{\mathbf{X}}(\mathbf{x})}}_{=1} \underbrace{\sum_{y_i} p_{Y_i}(y_i)}_{=1} \\ &+ \sum_{t=1}^T \sum_{i=1}^N \Pr(i(t) = i) \underbrace{\sum_{\mathbf{x}} p_{\mathbf{X}}(\mathbf{x})}_{=1} \underbrace{\sum_{y_i} p_{Y_i}(y_i) \log \frac{p_{Y_i}(y_i)}{p'_{Y_i}(y_i)}}_{=1} \\ &= T D_{\text{KL}}(p_{\mathbf{X}} \parallel p'_{\mathbf{X}}) + \sum_{i=1}^N D_{\text{KL}}(p_{Y_i} \parallel p'_{Y_i}) \sum_{t=1}^T \Pr(i(t) = i). \end{aligned} \quad (28)$$

□

We now prove Theorem 1.

Proof. Fix an arbitrary randomized policy (π) that achieves $R(T) = o(T^{\delta}) \quad \forall \delta > 0$ under 2/F/B feedback. Fix an arm $j \in \mathcal{I}$, i.e., $j \neq i^*$ with $\alpha_j > \alpha_{i^*} \beta_{i^*}$, and fix $\lambda \in (\Delta_j, \alpha_j(1 - \beta_j))$. We construct a new problem instance given by a second set of parameters $\boldsymbol{\alpha}'$ and $\boldsymbol{\beta}'$, where $\boldsymbol{\alpha}' = \boldsymbol{\alpha}$, $\beta'_j = \beta_j + \lambda/\alpha_j$, and $\beta'_i = \beta_i$ for all $i \neq j$. Note that setting $\lambda = \alpha_j(1 - \beta_j)$ gives $\beta'_j = 1$, and $\Delta_j < \alpha_j(1 - \beta_j)$ since $\alpha_j > \alpha_{i^*} \beta_{i^*}$. Then choosing any $\lambda \in (\Delta_j, \alpha_j(1 - \beta_j))$ indeed gives valid parameters $\alpha'_i, \beta'_i \in [0, 1]$ for all $i \in [N]$.

Observe that $\alpha'_j \beta'_j = \alpha_j \beta_j + \lambda > \alpha_{i^*} \beta_{i^*}$ and therefore $j \in \operatorname{argmax}_{i \in [N]} \alpha'_i \beta'_i$ is an optimal arm under the bandit setting with parameters $\boldsymbol{\alpha}'$, $\boldsymbol{\beta}'$ and the reward gaps $\Delta'_i \triangleq \alpha'_j \beta'_j - \alpha_i \beta_i$ satisfy

$$\Delta'_i = \alpha_j \beta_j + \lambda - \alpha_i \beta_i = \lambda - (\alpha_i \beta_i - \alpha_j \beta_j) \geq \lambda - \Delta_j, \quad \forall i \neq j. \quad (29)$$

Let \Pr' denote the probability measure and \mathbb{E}' denote the expectation operator in the setting with parameters $(\boldsymbol{\alpha}', \boldsymbol{\beta}')$, and let $R'(T) \triangleq T \alpha'_j \beta'_j - \sum_{t=1}^T \mathbb{E}'[Z_{i(t)}(t)]$ denote the cumulative regret in this setting. Then

$$\begin{aligned} R'(T) &= \sum_{i \neq j} \Delta'_i \mathbb{E}'[n_i(T)] \geq (\lambda - \Delta_j)(T - \mathbb{E}'[n_j(T)]), \\ R(T) &= \sum_{i \neq j} \Delta_i \mathbb{E}[n_i(T)] \geq \Delta_j \mathbb{E}[n_j(T)] \end{aligned} \quad (30)$$

Define the event $\mathcal{E} \triangleq \{n_j(T) < T/2\}$. Then from the above, we have $R'(T) \geq \frac{1}{2}(\lambda - \Delta_j)T \Pr'(\mathcal{E})$ and $R(T) \geq \frac{1}{2}\Delta_j T \Pr(\mathcal{E}^c)$. Therefore

$$R'(T) + R(T) \geq \frac{1}{2}T \min\{(\lambda - \Delta_j), \Delta_j\} [\Pr(\mathcal{E}^c) + \Pr'(\mathcal{E})]. \quad (31)$$

Using the same notation as Lemma 2, let p_π and p'_π denote the probability mass functions of the sequence of observations $(i(t), \mathbf{X}(t), Y_{i(t)}(t))_{t=1}^T$ when the policy (π) is used under the probability measures \Pr and \Pr' respectively. Note that $n_j(T)$ is a function of $(i(t), \mathbf{X}(t), Y_{i(t)}(t))_{t=1}^T$. Then we can write $\Pr(\mathcal{E}) = \sum_{\omega \in \mathcal{E}} p_\pi(\omega)$ (mutatis mutandis for $\Pr'(\mathcal{E})$) and therefore

$$\begin{aligned} \Pr(\mathcal{E}) - \Pr'(\mathcal{E}) &= \sum_{\omega \in \mathcal{E}} p_\pi(\omega) - \sum_{\omega \in \mathcal{E}} p'_\pi(\omega) \\ &\leq \sup_{\text{event } A} \left| \sum_{\omega \in A} p_\pi(\omega) - \sum_{\omega \in A} p'_\pi(\omega) \right| \\ &= D_{\text{TV}}(p_\pi, p'_\pi) \stackrel{(a)}{\leq} 1 - \frac{1}{2}e^{-D_{\text{KL}}(p_\pi \parallel p'_\pi)} \end{aligned} \quad (32)$$

where D_{TV} denotes the total variation distance and (a) applies the Bretagnolle-Huber inequality. Rearranging and using the fact that $\Pr(\mathcal{E}^c) = 1 - \Pr(\mathcal{E})$ gives

$$\begin{aligned} \Pr(\mathcal{E}^c) + \Pr'(\mathcal{E}) &\geq \frac{1}{2}e^{-D_{\text{KL}}(p_\pi \parallel p'_\pi)} \\ &\stackrel{(a)}{=} \frac{1}{2}e^{-D_{\text{KL}}(p_{Y_j} \parallel p'_{Y_j}) \mathbb{E}[n_j(T)]}, \end{aligned} \quad (33)$$

where (a) is from Lemma 2 (note that $D_{\text{KL}}(p_\mathbf{X} \parallel p'_{\mathbf{X}}) = 0$ since $\boldsymbol{\alpha} = \boldsymbol{\alpha}'$ and each $D_{\text{KL}}(p_{Y_i} \parallel p'_{Y_i}) = 0$ since $\beta_i = \beta'_i$ for $i \neq j$). Substituting (33) into (31) and rearranging gives

$$e^{D_{\text{KL}}(p_{Y_j} \parallel p'_{Y_j}) \mathbb{E}[n_j(T)]} \geq \frac{\frac{1}{2}T \min\{(\lambda - \Delta_j), \Delta_j\}}{R'(T) + R(T)}. \quad (34)$$

Taking the logarithm of both sides, dividing by $\log T$ and rearranging gives

$$\begin{aligned} \frac{\mathbb{E}[n_j(T)]}{\log T} &\geq \frac{1}{D_{\text{KL}}(p_{Y_j} \parallel p'_{Y_j})} + \frac{\log(\frac{1}{4} \min\{(\lambda - \Delta_j), \Delta_j\})}{D_{\text{KL}}(p_{Y_j} \parallel p'_{Y_j}) \log T} \\ &\quad - \frac{\log(R'(T) + R(T))}{D_{\text{KL}}(p_{Y_j} \parallel p'_{Y_j}) \log T}. \end{aligned} \quad (35)$$

Taking the limit inferior as $T \rightarrow \infty$ of both sides, we need only inspect the last term on the right-hand side. Recall that $R(T) = o(T^\delta) \quad \forall \delta > 0$. Then $\forall \delta > 0$, there exists a constant $C_\delta > 0$ such that $R'(T) + R(T) \leq C_\delta T^\delta$ and therefore

$$\limsup_{T \rightarrow \infty} \frac{\log(R'(T) + R(T))}{\log T} \leq \limsup_{T \rightarrow \infty} \frac{\log(C_\delta) + \delta \log T}{\log T} = \delta. \quad (36)$$

Since δ can be taken arbitrarily small and positive, it follows that

$$\limsup_{T \rightarrow \infty} \frac{\log(R'(T) + R(T))}{\log T} = 0. \quad (37)$$

and so $\liminf_{T \rightarrow \infty} \frac{\mathbb{E}[n_j(T)]}{\log T} \geq \frac{1}{D_{\text{KL}}(p_{Y_j} \parallel p'_{Y_j})}$. Since this holds for all $\lambda \in (\Delta_j, \alpha_j(1 - \beta_j)]$, taking the infimum over λ gives the result. \square

Appendix B Proof of Lemma 1

Before proceeding to the proof, we first introduce a key definition and a supporting lemma (cf. Lemma 3), whose proof is provided in Appendix C, to facilitate the analysis.

Definition 2. Define $p_{i^*,t}$ as the probability that the estimated weight of arm i^* is greater than $\alpha_{i^*} \beta_{i^*} - \epsilon_3$ given the history until $t-1$, i.e., $p_{i^*,t} \triangleq \Pr(\bar{\alpha}_{i^*}(t) \theta_{\beta,i^*}(t) > \alpha_{i^*} \beta_{i^*} - \epsilon_3 | \mathcal{F}_{t-1})$, where $\mathcal{F}_t \triangleq \{i(\tau), X_1(\tau), \dots, X_N(\tau), Y_{i(\tau)}(\tau), \tau = 1, \dots, t\}$.

Lemma 3. For all $t, i \neq i^*$, we have

$$\begin{aligned} \Pr(i(t) = i, E_i^\mu(t), E_i^\theta(t), E_{i^*}^\mu(t) | \mathcal{F}_{t-1}) \\ \leq \frac{(1 - p_{i^*,t})}{p_{i^*,t}} \Pr(i(t) = i^*, E_i^\mu(t), E_i^\theta(t), E_{i^*}^\mu(t) | \mathcal{F}_{t-1}). \end{aligned} \quad (38)$$

We now proceed with the proof of Lemma 1.

Proof. We first prove (11). Applying the law of total expectation followed by Lemma 3 to the LHS of (11) gives

$$\begin{aligned} &\sum_{t=1}^T \Pr(i(t) = i, E_i^\mu(t), E_i^\theta(t), E_{i^*}^\mu(t)) \\ &= \sum_{t=1}^T \mathbb{E}[\Pr(i(t) = i, E_i^\mu(t), E_i^\theta(t), E_{i^*}^\mu(t) | \mathcal{F}_{t-1})] \\ &\leq \sum_{t=1}^T \mathbb{E}\left[\frac{(1 - p_{i^*,t})}{p_{i^*,t}} \Pr\left(\begin{array}{|c|} \hline i(t) = i \\ \hline E_i^\mu(t) \\ \hline E_i^\theta(t) \\ \hline E_{i^*}^\mu(t) \\ \hline \end{array} \middle| \mathcal{F}_{t-1}\right)\right] \end{aligned}$$

$$\begin{aligned}
&\stackrel{(a)}{=} \sum_{t=1}^T \mathbb{E} \left[\mathbb{E} \left[\frac{(1-p_{i^*,t})}{p_{i^*,t}} \mathbb{1} \left(\begin{array}{c} i(t)=i^* \\ E_i^\theta(t) \\ E_i^\mu(t) \\ E_{i^*}^\mu(t) \end{array} \right) \middle| \mathcal{F}_{t-1} \right] \right] \\
&\stackrel{(b)}{=} \sum_{t=1}^T \mathbb{E} \left[\frac{(1-p_{i^*,t})}{p_{i^*,t}} \mathbb{1}(i(t)=i^*, E_i^\theta(t), E_i^\mu(t), E_{i^*}^\mu(t)) \right] \\
&= \sum_{t=1}^T \mathbb{E} \left[\left(\frac{1}{p_{i^*,t}} - 1 \right) \mathbb{1}(i(t)=i^*, E_i^\theta(t), E_i^\mu(t), E_{i^*}^\mu(t)) \right] \\
&= \mathbb{E} \left[\sum_{t=1}^T \left(\frac{1}{\Pr(\bar{\alpha}_{i^*}(t)\theta_{\beta,i^*}(t) > \alpha_{i^*}\beta_{i^*} - \epsilon_3 | \mathcal{F}_{t-1})} - 1 \right) \right. \\
&\quad \left. \cdot \mathbb{1}(i(t)=i^*, E_i^\theta(t), E_i^\mu(t)) \mathbb{1}(E_{i^*}^\mu(t)) \right] \\
&\stackrel{(c)}{\leq} \mathbb{E} \left[\sum_{t=1}^T \left(\frac{1}{\Pr(\theta_{\beta,i^*}(t) > \frac{\alpha_{i^*}\beta_{i^*}-\epsilon_3}{\alpha_{i^*}-\epsilon_2} | \mathcal{F}_{t-1})} - 1 \right) \right. \\
&\quad \left. \cdot \mathbb{1}(i(t)=i^*, E_i^\theta(t), E_i^\mu(t)) \mathbb{1}(E_{i^*}^\mu(t)) \right] \\
&\leq \mathbb{E} \left[\sum_{t=1}^T \left(\frac{1}{\Pr(\theta_{\beta,i^*}(t) > \frac{\alpha_{i^*}\beta_{i^*}-\epsilon_3}{\alpha_{i^*}-\epsilon_2} | \mathcal{F}_{t-1})} - 1 \right) \right. \\
&\quad \left. \cdot \mathbb{1}(i(t)=i^*) \right], \quad (39)
\end{aligned}$$

where step (a) is because $p_{i^*,t}$ is \mathcal{F}_{t-1} -measurable; (b) follows from the law of total expectation; (c) is because if $\mathbb{1}(E_{i^*}^\mu(t)) = 1$, we have $\bar{\alpha}_{i^*}(t) \geq \alpha_{i^*} - \epsilon_2$ and if $\mathbb{1}(E_{i^*}^\mu(t)) = 0$, the entire expression = 0.

For simplicity, we denote $x \triangleq \frac{\alpha_{i^*}\beta_{i^*}-\epsilon_3}{\alpha_{i^*}-\epsilon_2}$ and the below always holds almost surely for any arm $i \in [N]$ according to the conditional independence and the proof of [23, Theorem 36.2]:

$$\begin{aligned}
&\Pr(\theta_{\beta,i}(t) > x | \mathcal{F}_{t-1}) \\
&= \Pr(\theta_{\beta,i}(t) > x | \{i(\tau), Y_{i(\tau)}(\tau), \tau = 1, \dots, t-1\}) \quad (40) \\
&= \Pr(\theta_{\beta,i}(t) > x | S_{\beta,i}(t), F_{\beta,i}(t)).
\end{aligned}$$

We recall $\tau_{s,i}$ denotes the timeslot that arm i was played for the s -th time. Substituting (40) into (39) gives

$$\begin{aligned}
&\mathbb{E} \left[\sum_{t=1}^T \left(\frac{1}{\Pr(\theta_{\beta,i^*}(t) > x | \mathcal{F}_{t-1})} - 1 \right) \mathbb{1}(i(t)=i^*) \right] \\
&= \mathbb{E} \left[\sum_{t=1}^T \left(\frac{1}{\Pr(\theta_{\beta,i^*}(t) > x | S_{\beta,i^*}(t), F_{\beta,i^*}(t))} - 1 \right) \mathbb{1}(i(t)=i^*) \right] \\
&= \mathbb{E} \left[\sum_{s=0}^{n_{i^*}(T)} \sum_{t=\tau_{s,i^*}+1}^{\tau_{s,i^*+1} \wedge T} \left(\frac{1}{\Pr(\theta_{\beta,i^*}(t) > x | S_{\beta,i^*}(t), F_{\beta,i^*}(t))} - 1 \right) \mathbb{1}(i(t)=i^*) \right] \\
&\stackrel{(a)}{=} \mathbb{E} \left[\sum_{s=0}^{n_{i^*}(T)} \left(\frac{1}{\Pr(\theta_{\beta,i^*}(\tau_{s,i^*}+1) > x | S_{\beta,i^*}(\tau_s+1), F_{\beta,i^*}(\tau_s+1))} - 1 \right) \right. \\
&\quad \left. \cdot \sum_{t=\tau_{s,i^*}+1}^{\tau_{s,i^*+1} \wedge T} \mathbb{1}(i(t)=i^*) \right] \\
&\stackrel{(b)}{\leq} \mathbb{E} \left[\sum_{s=0}^{n_{i^*}(T)} \left(\frac{1}{\Pr(\theta_{\beta,i^*}(\tau_{s,i^*}+1) > x | S_{\beta,i^*}(\tau_{s,i^*}+1), F_{\beta,i^*}(\tau_{s,i^*}+1))} - 1 \right) \right] \\
&\stackrel{(c)}{\leq} \mathbb{E} \left[\left(\frac{1}{\Pr(\theta_{\beta,i^*}(\tau_{s,i^*}+1) > x | S_{\beta,i^*}(\tau_{s,i^*}+1), F_{\beta,i^*}(\tau_{s,i^*}+1))} - 1 \right) \right] \\
&\stackrel{(d)}{=} \sum_{s=0}^{T-1} \mathbb{E} \left[\left(\frac{1}{\Pr(\theta_{\beta,i^*}(\tau_{s,i^*}+1) > x | \mathcal{H}_{\tau_{s,i^*}})} - 1 \right) \right], \quad (41)
\end{aligned}$$

where step (a) is because for $t \in \{\tau_{s,i^*}+1, \dots, \tau_{s,i^*+1} \wedge T\}$, $\Pr(\theta_{\beta,i^*}(t) > x | S_{\beta,i^*}(t), F_{\beta,i^*}(t)) = \Pr(\theta_{\beta,i^*}(\tau_{s,i^*}+1) > x | S_{\beta,i^*}(\tau_{s,i^*}+1), F_{\beta,i^*}(\tau_{s,i^*}+1))$ almost surely; (b) is true since $i(t) = i^*$ only in timeslots $t = \tau_{s,i^*}$ for some $s > 0$; (c) follows the fact $n_{i^*}(T) \leq T-1$; (d) uses (40) and $\mathcal{H}_t \triangleq \{i(\nu), Y_{i(\nu)}(\nu), \nu = 1, \dots, t\}$.

To bound the expression in (41), we introduce the following lemma, which restates the result from [15, Lemma 2.9].

Lemma 4. For a given number of playing times s , the following holds for the optimal arm i^* with threshold $x < \beta_{i^*}$

$$\begin{aligned}
&\mathbb{E} \left[\frac{1}{\Pr(\theta_{\beta,i^*}(\tau_{s,i^*}+1) > x | \mathcal{H}_{\tau_{s,i^*}})} - 1 \right] \\
&\leq \begin{cases} \frac{3}{\Delta'} & s < \frac{8}{\Delta'} \\ \Theta \left(e^{-\Delta'^2 s/2} + \frac{1}{(s+1)\Delta'^2} e^{-Ds} + \frac{1}{e^{\Delta'^2 s/4} - 1} \right) & s \geq \frac{8}{\Delta'} \end{cases} \quad (42)
\end{aligned}$$

where $\Delta' = \beta_{i^*} - x$ and $D = d(x, \beta_{i^*}) = x \log \frac{x}{\beta_{i^*}} + (1-x) \log \frac{1-x}{1-\beta_{i^*}}$.

Crucially, the result in Lemma 4 characterizes an intrinsic property of the posterior distribution after s trials and is invariant to the arm playing policy. Under the Beta-Bernoulli update, the posterior distribution of arm i^* is uniquely determined by the sufficient statistics (the number of successes and failures), as shown in (40). Although our algorithm employs a specific strategy to select arm, given s trials, the number of successes and failures, i.e., $(S_{\beta,i^*}(\tau_{s,i^*}+1), F_{\beta,i^*}(\tau_{s,i^*}+1))$, is independent of the arm selection process $\{i(t)\}_{t=1,2,\dots,\tau_{s,i^*}}$. This decoupling ensures that the concentration properties of the posterior distribution remain identical to those analyzed in [15, Lemma 2.9].

After summing (42) over $s \in \{0, \dots, T-1\}$, we obtain

$$\begin{aligned} & \sum_{s=0}^{T-1} \mathbb{E} \left[\left(\frac{1}{\Pr(\theta_{\beta,i^*}(\tau_{s,i^*}+1) > x \mid \mathcal{H}_{\tau_{s,i^*}})} - 1 \right) \right] \\ & \leq \sum_{s < 8/\Delta'} \frac{3}{\Delta'} \\ & + \sum_{s \geq 8/\Delta'} \Theta \left(e^{-\Delta'^2 s/2} + \frac{1}{(s+1)\Delta'^2} e^{-Ds} + \frac{1}{e^{\Delta'^2 s/4} - 1} \right) \\ & \leq \frac{24}{\Delta'^2} + \Theta \left(\frac{1}{\Delta'^2} + \frac{1}{\Delta'^2 D} + \frac{1}{\Delta'^2} \ln \frac{1}{\Delta'} \right), \end{aligned} \quad (43)$$

where the last inequality follows from the arguments: (1) The sum $\sum_s e^{-\Delta'^2 s/2}$ is a geometric series with ratio $e^{-\Delta'^2/2}$. Its sum is bounded by $\frac{1}{1-e^{-\Delta'^2/2}} \approx \frac{2}{\Delta'^2}$ by using the approximation $1-e^{-x} \approx x$ for small x , contributing the $\Theta(1/\Delta'^2)$ term; (2) The sum $\sum_s e^{-Ds}$ is a geometric series with ratio e^{-D} . This yields $\frac{1}{\Delta'^2(1-e^{-D})} \approx \frac{1}{\Delta'^2 D}$, contributing the $\Theta(1/(\Delta'^2 D))$ term; (3) For the sum $\sum_s \frac{1}{e^{\Delta'^2 s/4} - 1}$, we use the integral upper bound for decreasing sequences: $\sum_{s=k}^{\infty} f(s) \leq f(k) + \int_k^{\infty} f(x) dx$. The integral evaluates to $\Theta(\frac{1}{\Delta'^2} \ln \frac{1}{\Delta'})$.

Inserting (43) into (41) and subsequently inserting into (39) gives

$$\begin{aligned} & \sum_{t=1}^T \Pr(i(t) = i, E_i^\mu(t), E_i^\theta(t), E_{i^*}^\mu(t)) \\ & \leq \frac{24}{\Delta'^2} + \Theta \left(\frac{1}{\Delta'^2} + \frac{1}{\Delta'^2 D} + \frac{1}{\Delta'^4} \right). \end{aligned} \quad (44)$$

Noticing that we can choose any $\epsilon_2 \in \Gamma_2$, the above gives

$$\begin{aligned} & \sum_{t=1}^T \Pr(i(t) = i, E_i^\mu(t), E_i^\theta(t), E_{i^*}^\mu(t)) \\ & \leq \inf_{\epsilon_2 \in \Gamma_2} \left(\frac{24}{\Delta'^2} + \Theta \left(\frac{1}{\Delta'^2} + \frac{1}{\Delta'^2 D} + \frac{1}{\Delta'^4} \right) \right), \end{aligned} \quad (45)$$

Next, we prove (12).

a) Case 1: $\alpha_i \geq \alpha_{i^*} \beta_{i^*}$: For arm $i \neq i^*$ satisfying $\alpha_i \geq \alpha_{i^*} \beta_{i^*}$, we can have

$$\begin{aligned} & \sum_{t=1}^T \Pr(i(t) = i, \overline{E_i^\theta(t)}, E_i^\mu(t)) \\ & = \sum_{t=1}^T \Pr(i(t) = i, n_i(t-1) \leq L_i(T), \overline{E_i^\theta(t)}, E_i^\mu(t)) \\ & + \sum_{t=1}^T \Pr(i(t) = i, n_i(t-1) > L_i(T), \overline{E_i^\theta(t)}, E_i^\mu(t)), \end{aligned} \quad (46)$$

where $L_i(T) = \frac{\log T}{d(\beta_i + \epsilon_1, \frac{\alpha_{i^*} \beta_{i^*} - \epsilon_3}{\alpha_i + \epsilon_1})}$.

The first term in (46) can be upper bounded as

$$\sum_{t=1}^T \Pr(i(t) = i, n_i(t-1) \leq L_i(T), \overline{E_i^\theta(t)}, E_i^\mu(t))$$

$$\begin{aligned} & = \sum_{t=1}^T \mathbb{E} \left[\mathbb{1} \left(i(t) = i, n_i(t-1) \leq L_i(T), \overline{E_i^\theta(t)}, E_i^\mu(t) \right) \right] \\ & = \mathbb{E} \left[\sum_{s=1}^{n_i(T)} \mathbb{1} \left(n_i(\tau_{s,i} - 1) \leq L_i(T), \overline{E_i^\theta(\tau_{s,i})}, E_i^\mu(\tau_{s,i}) \right) \right] \\ & = \mathbb{E} \left[\sum_{s=0}^{n_i(T)-1} \mathbb{1} \left(s \leq L_i(T), \overline{E_i^\theta(\tau_{s,i})}, E_i^\mu(\tau_{s,i}) \right) \right] \\ & \leq L_i(T) + 1. \end{aligned} \quad (47)$$

Then we focus on bounding the second term in (46).

$$\begin{aligned} & \sum_{t=1}^T \Pr(i(t) = i, n_i(t-1) > L_i(T), \overline{E_i^\theta(t)}, E_i^\mu(t)) \\ & = \sum_{t=1}^T \mathbb{E} \left[\mathbb{1} \left(i(t) = i, n_i(t-1) > L_i(T), \overline{E_i^\theta(t)}, E_i^\mu(t) \right) \right] \\ & \stackrel{(a)}{=} \mathbb{E} \left[\sum_{t=1}^T \mathbb{E} \left[\mathbb{1} \left(i(t) = i, n_i(t-1) > L_i(T), \overline{E_i^\theta(t)}, E_i^\mu(t) \right) \mid \mathcal{F}_{t-1} \right] \right] \\ & \stackrel{(b)}{=} \mathbb{E} \left[\sum_{t=1}^T \mathbb{1} \left(n_i(t-1) > L_i(T), E_i^\mu(t) \right) \Pr(i(t) = i, \overline{E_i^\theta(t)} \mid \mathcal{F}_{t-1}) \right] \\ & \leq \mathbb{E} \left[\sum_{t=1}^T \mathbb{1} \left(n_i(t-1) > L_i(T), |\bar{\alpha}_i(t) - \alpha_i| \leq \epsilon_1, |\bar{\beta}_i(t) - \beta_i| \leq \epsilon_1 \right) \right. \\ & \quad \left. \cdot \Pr(\bar{\alpha}_i(t) \theta_{\beta,i}(t) > \alpha_{i^*} \beta_{i^*} - \epsilon_3 \mid \mathcal{F}_{t-1}) \right], \end{aligned}$$

where step (a) uses the law of total expectation and (b) uses the fact that $\mathbb{1}(n_i(t-1) > L_i(T), E_i^\mu(t))$ is \mathcal{F}_{t-1} -measurable.

By definition, $S_{\beta,i}(t) = \bar{\beta}_i(t) n_i(t-1) + 1$, and therefore, $\theta_{\beta,i}(t)$ is a Beta $(\bar{\beta}_i(t) n_i(t-1) + 1, (1 - \bar{\beta}_i(t)) n_i(t-1) + 1)$ distributed random variable. Combing with (40) gives

$$\begin{aligned} & \Pr(\theta_{\beta,i}(t) > y \mid \mathcal{F}_{t-1}) \\ & = \Pr(\theta_{\beta,i}(t) > y \mid \bar{\beta}_i(t) n_i(t-1), (1 - \bar{\beta}_i(t)) n_i(t-1)). \end{aligned} \quad (48)$$

In addition, noting that a Beta(s, f) random variable is stochastically dominated by Beta(s', f') if $s' \geq s, f' \leq f$. Therefore, if $\bar{\beta}_i(t) \leq z$, the distribution of $\theta_{\beta,i}(t)$ is stochastically dominated by Beta($z n_i(t-1) + 1, (1 - z) n_i(t-1) + 1$). Therefore, given a sample path $\mathcal{F}_{t-1} = F_{t-1}$ such that $\{\bar{\beta}_i(t) \leq z\} \subseteq \{\mathcal{F}_{t-1} = F_{t-1}\}$, for any z , we have

$$\begin{aligned} & \Pr(\theta_{\beta,i}(t) > y \mid \mathcal{F}_{t-1} = F_{t-1}) \\ & \stackrel{(a)}{=} 1 - F_{\bar{\beta}_i(t) n_i(t-1) + 1, (1 - \bar{\beta}_i(t)) n_i(t-1) + 1}^{\text{Beta}}(y) \\ & \stackrel{(b)}{\leq} 1 - F_{z n_i(t-1) + 1, (1 - z) n_i(t-1) + 1}^{\text{Beta}}(y) \\ & \stackrel{(c)}{=} F_{n_i(t-1) + 1, y}^B(z n_i(t-1)), \end{aligned} \quad (49)$$

where step (a) uses (48); (b) uses the definition of first-order stochastic dominance; (c) uses the relationship between CDF of Beta distribution and that of Binomial

distribution $F_{\alpha,\beta}^{\text{beta}}(y) = 1 - F_{\alpha+\beta-1,y}^B(\alpha-1)$ for all positive integers α, β .

We only consider the sample path $\mathcal{F}_{t-1} = F_{t-1}$ such that $\{\bar{\alpha}_i(t) \leq \alpha_i + \epsilon_1\} \cap \{\bar{\beta}_i(t) \leq \beta_i + \epsilon_1\} \cap \{n_i(t) > L_i(T)\} \subseteq \{\mathcal{F}_{t-1} = F_{t-1}\}$ otherwise (48) is equal to zero. Fix a sample path $\mathcal{F}_{t-1} = F_{t-1}$ satisfying the aforementioned conditions, we can derive

$$\begin{aligned} & \Pr(\bar{\alpha}_i(t)\theta_{\beta,i}(t) > \alpha_{i^*}\beta_{i^*} - \epsilon_3 \mid \mathcal{F}_{t-1} = F_{t-1}) \\ & \leq \Pr\left(\theta_{\beta,i}(t) \geq \frac{\alpha_{i^*}\beta_{i^*} - \epsilon_3}{\alpha_i + \epsilon_1} \mid \mathcal{F}_{t-1} = F_{t-1}\right) \\ & \stackrel{(a)}{\leq} F_{n_i(t-1)+1, \frac{\alpha_{i^*}\beta_{i^*} - \epsilon_3}{\alpha_i + \epsilon_1}}^B((\beta_i + \epsilon_1)n_i(t-1)) \\ & \stackrel{(b)}{\leq} F_{n_i(t-1)+1, \frac{\alpha_{i^*}\beta_{i^*} - \epsilon_3}{\alpha_i + \epsilon_1}}^B((\beta_i + \epsilon_1)(n_i(t-1) + 1)) \\ & \stackrel{(c)}{\leq} e^{-(n_i(t-1)+1)d\left(\beta_i + \epsilon_1, \frac{\alpha_{i^*}\beta_{i^*} - \epsilon_3}{\alpha_i + \epsilon_1}\right)} \stackrel{(d)}{\leq} \frac{1}{T}, \end{aligned} \quad (50)$$

where step (a) uses (49) for $z = \beta_i + \epsilon_1$ since $\bar{\beta}_i(t) \leq z$ under the sample path $\mathcal{F}_{t-1} = F_{t-1}$; (b) follows from the fact that CDF of any random variable is non-decreasing; (c) uses the Chernoff-Hoeffding Bound; (d) from $n_i(t-1)+1 \geq n_i(t) > L_i(T)$.

Inserting (50) into (48) gives

$$\sum_{t=1}^T \Pr\left(i(t) = i, n_i(t-1) > L_i(T), \bar{E}_i^\theta(t), E_i^\mu(t)\right) \leq 1 \quad (51)$$

After substituting (47) and (51) into (46), for arm $i \neq i^*$ satisfying $\alpha_i \geq \alpha_{i^*}\beta_{i^*}$, we obtain

$$\sum_{t=1}^T \Pr\left(i(t) = i, \bar{E}_i^\theta(t), E_i^\mu(t)\right) \leq \frac{\log T}{d(\beta_i + \epsilon_1, \frac{\alpha_{i^*}\beta_{i^*} - \epsilon_3}{\alpha_i + \epsilon_1})} + 1. \quad (52)$$

Since the above holds for any $\epsilon_1 \in \Gamma_1$, we further arrive

$$\begin{aligned} & \sum_{t=1}^T \Pr\left(i(t) = i, \bar{E}_i^\theta(t), E_i^\mu(t)\right) \\ & \leq \inf_{\epsilon_1 \in \Gamma_1} \frac{\log T}{d(\beta_i + \epsilon_1, \frac{\alpha_{i^*}\beta_{i^*} - \epsilon_3}{\alpha_i + \epsilon_1})} + 1. \end{aligned} \quad (53)$$

b) Case 2: $\alpha_i < \alpha_{i^*}\beta_{i^*}$: For arm $i \neq i^*$ satisfying $\alpha_i < \alpha_{i^*}\beta_{i^*}$, we can choose any $\epsilon_4 \in \Gamma_4 \triangleq (0, \alpha_{i^*}\beta_{i^*} - \alpha_i - \epsilon_3)$ such that

$$\begin{aligned} & \sum_{t=1}^T \Pr\left(i(t) = i, \bar{E}_i^\theta(t), E_i^\mu(t)\right) \\ & = \sum_{t=1}^T \Pr(i(t) = i, \bar{\alpha}_i(t)\theta_{\beta,i}(t) > \alpha_{i^*}\beta_{i^*} - \epsilon_3, E_i^\mu(t)) \\ & \leq \sum_{t=1}^T \Pr(\bar{\alpha}_i(t) \geq \alpha_i + \epsilon_4) \\ & \stackrel{(a)}{\leq} 1 + \sum_{t=1}^{\infty} \exp(-td(\alpha_i + \epsilon_4, \alpha_i)) \stackrel{(b)}{\leq} 1 + \frac{1}{2\epsilon_4^2}, \end{aligned} \quad (54)$$

where step (a) uses the Chernoff-Hoeffding bound; (b) uses the Pinsker inequality.

Therefore, for arm $i \neq i^*$ satisfying $\alpha_i < \alpha_{i^*}\beta_{i^*}$, we obtain

$$\sum_{t=1}^T \Pr\left(i(t) = i, \bar{E}_i^\theta(t), E_i^\mu(t)\right) \leq \inf_{\epsilon_4 \in (0, \alpha_{i^*}\beta_{i^*} - \alpha_i - \epsilon_3)} \frac{1}{2\epsilon_4^2} + 1. \quad (55)$$

After combining Case 1 and Case 2, (12) can be proved.

Then we utilize the following to prove (13). For $i \neq i^*$,

$$\begin{aligned} & \sum_{t=1}^T \Pr\left(i(t) = i, \bar{E}_i^\mu(t)\right) \\ & \stackrel{(a)}{\leq} 1 + \sum_{l=2}^T \Pr\left(\bar{E}_i^\mu(\tau_{l,i})\right) \\ & \stackrel{(b)}{\leq} 1 + \sum_{l=2}^T \Pr(|\bar{\alpha}_i(\tau_{l,i}) - \alpha| > \epsilon_1) + \sum_{l=2}^T \Pr(|\bar{\beta}_i(\tau_{l,i}) - \beta| > \epsilon_1) \\ & \stackrel{(c)}{\leq} 1 + \sum_{l=1}^{\infty} \exp(-ld(\alpha_i - \epsilon_1, \alpha_i)) + \sum_{l=1}^{\infty} \exp(-ld(\alpha_i + \epsilon_1, \alpha_i)) \\ & \quad + \sum_{l=1}^{\infty} \exp(-ld(\beta_i - \epsilon_1, \beta_i)) + \sum_{l=1}^{\infty} \exp(-ld(\beta_i + \epsilon_1, \beta_i)) \\ & \stackrel{(d)}{\leq} 1 + \frac{2}{\epsilon_1^2}, \end{aligned} \quad (56)$$

where step (a) uses the definition of $\tau_{l,i}$; (b) uses the Union Bound; (c) and (d) are similar to (a) and (b) in (54).

Then we can prove (14) since

$$\begin{aligned} \sum_{t=1}^T \Pr\left(\bar{E}_{i^*}^\mu(t)\right) & \leq 1 + \sum_{t=2}^T \Pr\left(\bar{E}_{i^*}^\mu(t)\right) \\ & = 1 + \sum_{t=2}^T \Pr(|\bar{\alpha}_{i^*}(t) - \alpha_{i^*}| > \epsilon_2) \\ & \stackrel{(a)}{\leq} 1 + \sum_{t=1}^{\infty} \exp(-td(\alpha_{i^*} - \epsilon_2, \alpha_{i^*})) \\ & \quad + \sum_{t=1}^{\infty} \exp(-td(\alpha_{i^*} + \epsilon_2, \alpha_{i^*})) \\ & \stackrel{(b)}{\leq} 1 + \frac{1}{\epsilon_2^2}, \end{aligned} \quad (57)$$

where (a) and (b) are similar to (a) and (b) in (54). \square

Appendix C Proof of Lemma 3

Proof. We will show that the inequality holds for any sample path $\mathcal{F}_{t-1} = F_{t-1}$. Note that $E_i^\mu(t)$ and $E_{i^*}^\mu(t)$ belong to the σ -algebra generated by \mathcal{F}_{t-1} . We can ignore any sample path $\mathcal{F}_{t-1} = F_{t-1}$ such that $E_i^\mu(t) \cap E_{i^*}^\mu(t) \not\subseteq \{\mathcal{F}_{t-1} = F_{t-1}\}$ since in that case,

$$\Pr(i(t) = i, E_i^\mu(t), E_i^\theta(t), E_{i^*}^\mu(t) \mid \mathcal{F}_{t-1} = F_{t-1}) = 0 \quad (58)$$

and the desired inequality is trivially true. Then fix a sample path $\mathcal{F}_{t-1} = F_{t-1}$ such that $E_i^\mu(t) \cap E_{i^*}^\mu(t) \subseteq \{\mathcal{F}_{t-1} = F_{t-1}\}$. Then for each $j \in \{i, i^*\}$, we have

$$\begin{aligned} & \Pr(i(t) = j, E_i^\mu(t), E_{i^*}^\mu(t) \mid \mathcal{F}_{t-1} = F_{t-1}) \\ &= \Pr(i(t) = j, E_i^\theta(t) \mid \mathcal{F}_{t-1} = F_{t-1}) \\ &= \Pr(i(t) = j \mid E_i^\theta(t), \mathcal{F}_{t-1} = F_{t-1}) \Pr(E_i^\theta(t) \mid \mathcal{F}_{t-1} = F_{t-1}). \end{aligned} \quad (59)$$

After plugging the above into (38), and dividing both sides by $\Pr(E_i^\theta(t) \mid \mathcal{F}_{t-1} = F_{t-1})$, it suffices to prove that

$$\begin{aligned} & \Pr(i(t) = i \mid E_i^\theta(t), \mathcal{F}_{t-1} = F_{t-1}) \\ & \leq \frac{(1 - p_{i^*,t}(F_{t-1}))}{p_{i^*,t}(F_{t-1})} \Pr(i(t) = i^* \mid E_i^\theta(t), \mathcal{F}_{t-1} = F_{t-1}). \end{aligned} \quad (60)$$

For any $i \neq i^*$,

$$\begin{aligned} & \Pr(i(t) = i \mid E_i^\theta(t), \mathcal{F}_{t-1} = F_{t-1}) \\ & \stackrel{(a)}{\leq} \Pr(\bar{\alpha}_j(t)\theta_{\beta,j}(t) \leq \alpha_{i^*}\beta_{i^*} - \epsilon_3, \forall j \mid E_i^\theta(t), \mathcal{F}_{t-1} = F_{t-1}) \\ & \stackrel{(b)}{=} \Pr(\bar{\alpha}_{i^*}(t)\theta_{\beta,i^*}(t) \leq \alpha_{i^*}\beta_{i^*} - \epsilon_3 \mid \mathcal{F}_{t-1} = F_{t-1}) \\ & \quad \cdot \Pr(\bar{\alpha}_j(t)\theta_{\beta,j}(t) \leq \alpha_{i^*}\beta_{i^*} - \epsilon_3, \forall j \neq i^* \mid E_i^\theta(t), \mathcal{F}_{t-1} = F_{t-1}) \\ &= \Pr(\bar{\alpha}_j(t)\theta_{\beta,j}(t) \leq \alpha_{i^*}\beta_{i^*} - \epsilon_3, \forall j \neq i^* \mid E_i^\theta(t), \mathcal{F}_{t-1} = F_{t-1}) \\ & \quad \cdot (1 - p_{i^*,t}(F_{t-1})), \end{aligned}$$

where (a) is by definition of the event $E_i^\theta(t)$ and because $\bar{\alpha}_j(t)\theta_{\beta,j}(t) \leq \bar{\alpha}_i(t)\theta_{\beta,i}(t)$ for all j when $i(t) = i$ by definition of the algorithm, and (b) is by defining the event $B = \{\bar{\alpha}_j(t)\theta_{\beta,j}(t) \leq \alpha_{i^*}\beta_{i^*} - \epsilon_3, \forall j \neq i^*\}$ and $B^* = \{\bar{\alpha}_{i^*}(t)\theta_{\beta,i^*}(t) \leq \alpha_{i^*}\beta_{i^*} - \epsilon_3\}$ and noticing that

$$\begin{aligned} & \Pr(B, B^* \mid E_i^\theta(t), \mathcal{F}_{t-1} = F_{t-1}) \\ &= \Pr(B^* \mid B, E_i^\theta(t), \mathcal{F}_{t-1} = F_{t-1}) \Pr(B \mid E_i^\theta(t), \mathcal{F}_{t-1} = F_{t-1}) \\ &= \Pr(B^* \mid \mathcal{F}_{t-1} = F_{t-1}) \Pr(B \mid E_i^\theta(t), \mathcal{F}_{t-1} = F_{t-1}) \end{aligned} \quad (61)$$

since the event B^* is conditionally independent from $B \cap E_i^\theta(t)$ given $\{\mathcal{F}_{t-1} = F_{t-1}\}$.

Similarly,

$$\begin{aligned} & \Pr(i(t) = i^* \mid E_i^\theta(t), \mathcal{F}_{t-1} = F_{t-1}) \\ & \geq \Pr(\bar{\alpha}_j(t)\theta_{\beta,j}(t) \leq \alpha_{i^*}\beta_{i^*} - \epsilon_3 < \bar{\alpha}_{i^*}(t)\theta_{\beta,i^*}(t), \\ & \quad \forall j \neq i^* \mid E_i^\theta(t), \mathcal{F}_{t-1} = F_{t-1}) \\ &= \Pr(\alpha_{i^*}\beta_{i^*} - \epsilon_3 < \bar{\alpha}_{i^*}(t)\theta_{\beta,i^*}(t) \mid \mathcal{F}_{t-1} = F_{t-1}) \\ & \quad \cdot \Pr(\bar{\alpha}_j(t)\theta_{\beta,j}(t) \leq \alpha_{i^*}\beta_{i^*} - \epsilon_3, \forall j \neq i^* \mid E_i^\theta(t), \mathcal{F}_{t-1} = F_{t-1}) \\ &= \Pr(\bar{\alpha}_j(t)\theta_{\beta,j}(t) \leq \alpha_{i^*}\beta_{i^*} - \epsilon_3, \forall j \neq i^* \mid E_i^\theta(t), \mathcal{F}_{t-1} = F_{t-1}) \\ & \quad \cdot p_{i^*,t}(F_{t-1}). \end{aligned}$$

Combining the above two inequalities, we get the desired result. \square